# Accepted Manuscript


Structure based medicinal chemistry-driven strategy to design substituted dihydropyrimidines as potential antileishmanial agents

Umer Rashid, Riffat Sultana, Nargis Shaheen, Syed Fahad Hassan, Farhana Yaqoob, Muhammad Jawad Ahmad, Fatima Iftikhar, Nighat Sultana, Saba Asghar, Masoom Yasinzai, Farzana Latif Ansari, Naveeda Akhter Qureshi

PII: S0223-5234(16)30196-9

DOI: 10.1016/j.ejmech.2016.03.022

Reference: EJMECH 8447

To appear in: *European Journal of Medicinal Chemistry*

Received Date: 22 May 2015

Revised Date: 8 March 2016

Accepted Date: 9 March 2016

Please cite this article as: U. Rashid, R. Sultana, N. Shaheen, S.F. Hassan, F. Yaqoob, M.J. Ahmad, F. Iftikhar, N. Sultana, S. Asghar, M. Yasinzai, F.L. Ansari, N.A. Qureshi, Structure based medicinal chemistry-driven strategy to design substituted dihydropyrimidines as potential antileishmanial agents, *European Journal of Medicinal Chemistry* (2016), doi: 10.1016/j.ejmech.2016.03.022.

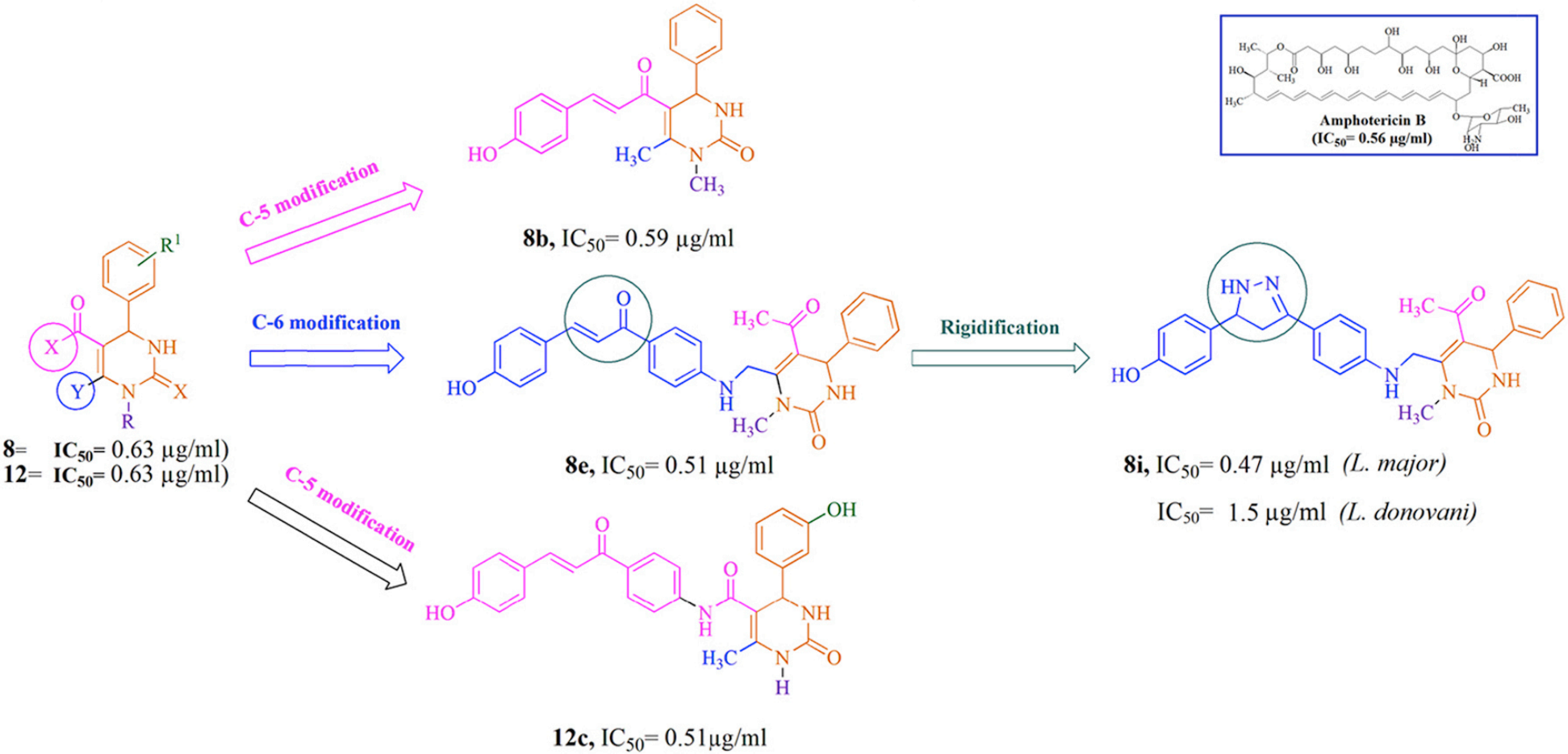
Amphotericin B
(IC50= 0.56 µg/ml)
C-5 modification
8b, IC50= 0.59 µg/ml
C-6 modification
8e, IC50= 0.51 µg/ml
Rigidification
8i, IC50= 0.47 µg/ml (L. major)
IC50= 1.5 µg/ml (L. donovani)
C-5 modification
12c, IC50= 0.51µg/ml
8= IC50= 0.63 µg/ml)
12= IC50= 0.63 µg/ml)

# Structure based medicinal chemistry-driven strategy to design substituted dihydropyrimidines as potential antileishmanial agents

Umer Rashid [a,b,*], Riffat Sultana [a], Nargis Shaheen [c], Syed Fahad Hassan [d], Farhana Yaqoob [a], Muhammad Jawad Ahmad [a], Fatima Iftikhar [a], Nighat Sultana [e], Saba Asghar [f], Masoom Yasinzai [f], Farzana Latif Ansari [g,h], Naveeda Akhter Qureshi [c, **]

[a] Department of Chemistry, Hazara University, Mansehra 21120, Pakistan

[b] Department of Chemistry, COMSATS Institute of Information Technology, Abbottabad 22060, Pakistan

[c] Department of Animal Sciences, Quaid-i-Azam University, Islamabad 45320, Pakistan

[d] Department of Pharmacy, University of Lahore, Defence Road Campus, Lahore 53700, Pakistan

[e] Department of Biochemistry, Hazara University, Mansehra 21120, Pakistan

[f] Department of Biochemistry, Quaid-i-Azam University, Islamabad 45320, Pakistan

[g] Department of Chemistry, Quaid-i-Azam University, Islamabad 45320, Pakistan

[h] Pakistan Council for Science and Technology, G-5/2 Islamabad, Pakistan

Corresponding author. *E-mail: umerrashid@ciit.net.pk; umer_rashid39@hotmail.com (Umer Rashid);

Tel. Off.: +92 (992) 383591-6

**E-mail: nqureshi@qau.edu.pk (NA Qureshi)

**Abstract**

In an attempt to explore novel and more potent antileishmanial compounds to diversify the current inhibitors, we pursued a medicinal chemistry-driven strategy to synthesize novel scaffolds with common pharmacophoric features of dihydropyrimidine and chalcone as current investigational antileishmanial compounds. Based on the reported X-ray structure of *Pteridine reductase 1* (PTR1) from *L. major*, we have designed a number of dihydropyrimidine-based derivatives to make specific interactions in PTR1 active site. Our lead compound **8i** has shown potent *in vitro* antileishmanial activity against promastigotes of *L. Major* and *L. donovani* with $IC_{50}$ value of 0.47 µg/ml and 1.5 µg/ml respectively. The excellent *in vitro* activity conclusively revealed that our lead compound is efficient enough to eradicate both visceral and topical leishmaniasis. In addition, docking analysis and *in silico* ADMET predictions were also carried out. Predicted molecular properties supported our experimental analysis that these compounds have potential to eradicate both visceral and topical leishmaniasis.

**Key words**: Leishmaniasis, Structure based drug design, Chalcones, Dihydropyrimidine, Docking, Rigidification

## 1. Introduction

Leishmaniasis is an infectious disease caused by *Leishmania* parasites belonging to genus Leishmania in the family Trypanosomatidae. It is transmitted into host blood by the bite of female sand fly [1]. These parasites can attack on mammals and human beings. When sandfly bites an infected organism parasite pass from the blood of infected organism into the gut of the sandfly. These parasites grow in the gut of sandfly for 8-20 days. When an infected sandfly bites a healthy organism it delivers these parasites (metacyclicpromastigote) in the blood of that organism. The infected stage, metacyclicpromastigotes inoculated in the rupture skin where it is phagocytosed by macrophages. The promastigotes multiplies and turn into amastigotes and infect many tissues which gradually express the disease. There are more than 20 Leishmanial protozoan species, that are responsible for a number of clinical forms of leishmaniasis such as cutaneous, diffuse cutaneous, disseminated cutaneous, mucocutaneous, visceral and post-kala-azar dermal leishmaniasis (PKDL). Leishmaniasis has many symptoms, such as destructive mucosal inflammation, skin lesions, ulcer and visceral infection (effects internal organs such as liver and spleen), fever and sometime anemia. This disease is prevalent in 88 countries, including Asia, Africa and Latin America. Visceral leishmaniasis (VL) is the most devastating and fatal form of leishmaniasis. It is caused by *L. donovani* and *L. infantum*. VL patients are prone to bacterial co-infection including tuberculosis and pneumonia etc. Post-kala-azar dermal leishmaniasis (PKDL), a form of dermal leishmaniasis caused by *L. donovani*, is a sequel of VL and develops months to years in VL cure patients [2].

In recent years, a plethora of investigational compounds has been investigated for antileishmanial activity. The major approved antileishmanial drugs are: pentavalent antimony drugs (meglumine antimoniate and sodium stibogluconate), pentamidine, miltefosine and amphotericin B. All these available treatments are not satisfactorily significant and have many draw backs such as renal dysfunction, nausea, anorexia, fever etc. There are also some reports of cardiac deaths. Besides investigational drugs, natural products are valuable sources in finding lead compounds. Flavonoids such as quercetin and luteolin emerged as potent antileishmanial agents against *L. donovani*. Similarly, natural products like lichochalcone A, iridoids, naphtoquinones, quinolone alkaloids, saponins, lignans and coumarins have shown promising antileishmanial activities [3-5]. Immunotherapy is considered as best alternative for the treatment of VL. Despite intense attempts to develop a prophylactic vaccine, there is no safe and efficacious vaccine against leishmaniasis due to inadequate knowledge of early immune response and poor understanding of parasite pathogenesis. However, Leish-111f+MPL-SE vaccine has been proved promising to control VL [6-7]. Apart from chemotherapy/vaccination, leishmaniasis can be controlled by taking some safety measures like reservoir eradication, use of insect repellent, protective clothing and use of fine-mesh netting to prevent exposure to female sand fly [8].

Chalcones (1,3-diaryl-2-propen-1-ones), belonging to the flavonoid family, have been reported to possess many pharmacological activities . Zhai et al reported oxygenated chalcones as potent inhibitors of *L. major* with $IC_{50}$ in the range of 4.0-10.5 mM [3]. Foroumadi et al investigated chromene-based chalcones namely, 1-(6-methoxy-2H-chromen-3-yl)3-phenylpropen-1-ones and 3-(6-methoxy-2H-chromen-3-yl)-1-phenyl-propen-1-ones for their antileishmanial activity against promastigotes form of Leishmania major [9]. These chalcones exhibited excellent activity at non-cytotoxic concentrations. Narender et al. reported promising antileishmanial activity of naturally occurring chromenochalcones [10]. 3,4-Dihydropyrimidine (DHPM) is the most attractive derivative of pyrimidines for a medicinal chemist. This structural motif may also be described as a derivative of cyclic urea. These non-planar heterocyclic compounds have received considerable attention of the pharmaceutical industry because of their interesting multifaceted pharmacological profiles. In the exploration of new and more potent antileishmanial compounds to diversify the current inhibitors, it is essential to design novel and potent inhibitors. Singh et al. identified potent dihydropyrimidine (DHPM) based derivatives targeting *Pteridine reductase* (PTR1) [11-12]. Recently, Kaur et al. reported monastrol, a dihydropyrimidine based KSP inhibitor, as a potent antileishmanial agent [13].

In our group, a major part of our research is focused on computer-aided drug design with subsequent synthesis and testing of new chemical entities as putative drugs for the treatment of various diseases [14-16]. Our group recently identified a series of N-(1-methyl-1H-indol-3-yl)methyleneamines and eight new 3,3-diaryl-4-(1-methyl-1Hindol-3-yl)azetidin-2-ones against Leishmania major [17]. In another study, we identified a variety of 2-aryl- and 5-nitro-2-arylbenzimidazoles as new antileishmanial agents with $IC_{50}$ values ranging from 0.62-0.92 µg/ml [18]. In continuation of our endeavor and considering the pharmacological importance of DHPM scaffold, it was planned to design and synthesize a variety of DHPM-based potent antileishmanial compounds to diversify the current inhibitors.

## 2. Results and discussion

### 2.1. The Design strategy

Molecular docking has contributed a lot in the identification of novel small drug-like scaffolds exhibiting high binding affinity and selectivity for the target. Hence, we extended our study to investigate in silico binding orientation of the synthesized DHPMs. *Pteridine reductase* (PTR1) is an important enzyme responsible for Pteridine salvage in leishmania and other trypanosomatid protozoans. PTR1 contributes to antifolate resistance and is responsible for the failure of conventional therapies such as methotrexate (MTX) against these protozoans [19]. In a study, Singh et al. reported DHPM analogues targeting PTR1, therefore, we focused on molecular docking studies to investigate PTR1 (from *L. major)* as a possible target for our newly synthesized DHPM derivatives. Crystal structure of PTR1 (PDB ID 1E7W, from *L. major*) with MTX as the co-crystallized ligand was selected for these studies [20]. Docking experiments were performed *via* Molecular Operating Environment (MOE) docking program [21].

**Table 1** enlists the 50% inhibitory concentration ($IC_{50}$) values of dihydropyrimidines (**1-13**). Compounds **1–13** showed varying degrees of antileishmanial activities with $IC_{50}$ values ranging between 0.61 and 0.99 µg/ml as compared to standard amphotericin B ($IC_{50}$= 0.56 µg/ml). Compound **3** ($IC_{50}$= 0.61±0.01), **4** ($IC_{50}$= 0.67±0.04 µg/ml), **8** ($IC_{50}$= 0.63±0.02 µg/ml), **12** ($IC_{50}$= 0.63±0.01 µg/ml), **13** ($IC_{50}$= 0.65±0.04 µg/ml) and were found to show good *in vitro* activity against the promastigote form of *L. Major*. Compounds **6** ($IC_{50}$= 0.71±0.01µg/ml), **7** ($IC_{50}$= 0.69±0.01µg/ml) and **9** ($IC_{50}$= 0.74±0.04µg/ml) exhibited moderate activities. Compounds **1**, 2, **5, 10** and **11** showed weak activities with $IC_{50}$ values between 0.78 and 0.89 µg/ml.

Active site of PTR1 is an elongated and rigid cleft. Arg17, Asn109, Ser111, Phe113, Asp181, Met183, Gln186, Leu188, Tyr194, Lys198, His241 are catalytically important residues (**Figure 1A-C**). Docking analysis of compound **8** with $IC_{50}$= 0.63±0.02 µg/ml was performed and our analysis identified unoccupied space, which may be available to attract further modifications. Superimposed model of compound **8** with MTX into the binding site of PTR1 (as viewed in Chimera 1.8.1) [22] is shown in **Figure 1A, B**. It is revealed from **Figure 1C** that pteridine head group of MTX is embedded between Met183, Gln186 and Leu188 and formed interactions with Gln186 at the distance of 1.4 Å (**Figure 1B**). While the glutamate tail accepted proton from Arg17 and Lys198. Phe113 forms π-stacking interactions with phenyl ring of *para*-aminobenzoate (*p*ABA)-glutamate tail (**Figure 1C**). The structure of compound **8** bound to PTR1 binding site showed that carbonyl oxygen of the cyclic urea act as a strong hydrogen bond acceptor and formed hydrogen bond with Lys198. Similarly, carbonyl oxygen of the C-5 acetyl group accepts hydrogen bond from Arg17 (**Figure 1D**). The observed negative fitness value of binding interaction (-8.9001 Kcal/mol) revealed that compound **8** was not tightly fitted into the active site. The orientation of MTX and its hydrogen bonding and π-stacking interactions provide a framework for the novel scaffold design. On the basis of these initial results, further molecular modeling, synthesis and *in vitro* PTR1 inhibition studies of compound **8** and **12** were carried out.

We realized that compound **8** can be chose as a benchmark compound for structural modification and both lipophilic and polar groups can be incorporated to probe extra binding interactions with the drug target. For this purpose, we turned our attention to further decorate DHPM scaffold by varying substituents around DHPM **8** to generate additional interactions with the drug target (**Series 1**). More specifically, we focused on a well-established chain extension strategy of medicinal chemistry which involves the incorporation of another functional group in the lead compound to enhance extra binding interactions with the PTR1. Based on the input from docking studies (**See below**), we designed analogues by varying substituent at C-5 and C-6 positions. Starting from C-5 acetyl group modification, a set of 5-cinnamoyl derivatives was synthesized in an effort to increase the potency (**Table 2**, Compounds **8a-c**). Additionally**,** substitution at C-6 position with 4-aminochalcone derivatives (**8d-i**) and the effect of placing 4-aminochalcone group at C-5 position of thioxo-analogues (Compound **12a-d**, $IC_{50}$=0.63±0.01) were also explored.

**2.2. Chemistry**

Dihydropyrimidines (**1-13**) were synthesized by using three component Biginelli reaction. Aldehydes, 1,3-dicarbonyl compounds and urea/thiourea were reacted in a test tube under ultrasonic irradiation by using $SnCl_2$ as catalyst and acetonitrile (ACN) as solvent (Scheme 1) [14]. DHPM **3** and **8**, having acetyl group at C-5 position, can undergo Claisen-Schmidt condensation with appropriate aldehydes to form chalcones. Furthermore, these may serve as versatile synthons capable of undergoing facile allylic bromination at C-6, which may undergo nucleophilic displacement with 4-amino chalcones or with any other nucleophile. Kolsov et al. studied effect of tautomerism in these two reactions and concluded that by inserting an alkyl substituent at N-1 position not only increased the solubility but also eliminated the possibility of amide-imidol tautomerism [23-24]. Based on these results, we initially started our investigation at C-5 position of N-methyl DHPM **8** and a set of three 5-cinnamoyl-6-methyl-4-aryl-3,4-dihydropyrimidin-2(1H)-one (**8a-c**) derivatives were synthesized by using Claisen-Schmidt condensation conditions (**Scheme 2**). The structures of synthesized compounds were confirmed on the basis of their physical constants and spectral data. $^1$H NMR data of 5-cinnamoyl derivatives revealed the absence of C-5 acetyl protons and showed two deshielded doublets, one proton integration each, appeared at 7.79-7.89 ppm and 7.56-7.59 ppm which could be assigned to olefinic protons of α, β-unsaturated ketone. Their coupling constant (*J*= 15.6-15.9 Hz) indicated the trans-relationship of H-α and H-β and hence confirming *E*-configuration of the compounds.

During one-pot Biginelli reaction, methyl group is generally introduced at C-6 position of the pyrimidine ring by using a 1,3-dicarbonyl compound essentially having an acyl group. This methyl group can undergo a facile bromination, described as allylic bromination, which may undergo nucleophilic substitution reaction leading to C-6 modified DHPMs. Allylic bromination was carried out at low temperature (0°C) in chloroform. The composition of crude reaction mixtures was monitored by LC/MS. In the chromatograms of the initial reaction mixture, peaks of 6-methyl brominated product (**19A**), 5-bromo acetyl product (**19B**) along with some di-brominated products was observed. The main peak (83%) corresponds to **19A.** These results were consistent with results reported in the literature [24]. The mixture of compounds was separated through standard silica gel column chromatography using n-hexane/ethyl acetate mixture as eluent. A mixture of 6-bromomethyl derivative of DHPM and 4′-aminochalcones (**14-18, Scheme 3a**) in THF were stirred in ultrasonic bath at the 40-45$^o$C to yield products (**8d-h, Scheme 3b**).

Rigidification has been an important medicinal chemistry tactic used to increase the activity of drug. Number of rotatable bonds measures molecular flexibility. Considering this medicinal chemistry approach, we decided to rigidify the Compound **8e** by converting chalcone (rotatable bonds=8) moiety to a five-membered pyrazoline ring (**8i**, rotatable bonds=7) (**Scheme 4**). Synthesis of pyrazoline **8i** involved [3+2] annulation of enone functionality of chalcone **8e** by reaction with hydrazine and NaOH [25]. A pale yellow colored solid was obtained by ultrasonic assisted reaction of chalcone with hydrazine and NaOH in 51% yield. In $^1$H NMR spectrum, an AMX pattern was observed. $H_A$, $H_M$ and $H_X$ protons of pyrazoline ring

appeared as doublets of a doublet at 4.81 ppm (*J*=12.3 Hz, 7.8 Hz) 3.93 (*J*=17.1 Hz, 12.3 Hz) and 3.44 (*J*=7.8 Hz, 17.1 Hz) ppm. The appearance of a downfield broad signal at 9.10 ppm was noticed for the phenolic-OH. In $^{13}$C-NMR spectra, C-4 and C-5 of pyrazoline ring appeared at 45.6 ppm and 56 ppm respectively.

We also synthesized a new series of thioxo-analogues by substituting C-5 ethyl ester group with 4-amino chalcone. This nucleophillic displacement reaction was carried out with 4-amino chalcones (**14-18**, Scheme **3a**) in THF in ultrasonic bath at 40-45$^{o}$C to yield products (**12a-d**). The synthesized compounds were characterized on the basis of their physical constants and spectral data. $^{1}$H NMR data of new thioxo-analogues were recorded, and a few generalizations could be made. Absence of signals of C-5 ethyl ester (a triplet at 1.09-1.14 ppm and a quartet at 4.01-4.10 ppm) and observation of a broad singlet, appeared at 9.23-9.27 ppm, was attributed to C-5 amide proton (N*H*-C=O) and was a clear indication of substitution reaction. Similarly, two deshielded doublets, one proton integration each, appeared at 7.99-8.04 ppm and 7.61-7.63 ppm which could be assigned to olefinic protons of α, β-unsaturated ketone.

### 2.3. *In vitro* antileishmanial assay

Substitution at C-5 gave a comparable potency to lead compound **DHPM 8**. The presence of a nitro group at 3-position of phenyl ring (**8a**) exhibited lower *in vitro* inhibition. However, compounds with hydroxyl and chlorine group at 4-position of phenyl ring (**8b** & **c** respectively) have shown similar potency to DHPM **8.** The results are summarized in Table **2**. Furthermore, substitution at C-6 position with 4-aminochalcone derivatives resulted in significant influence on antileishmanial activity with an $IC_{50}$ values ranging from 0.51 to 0.71 µg/ml. As shown in **Table 2**, chalcone derivative **8f** with nitro group at 3-position of phenyl ring has shown reduced potency. Similarly, derivative **8h** with 4-dimethtlamino group also exhibited reduced potency with $IC_{50}$ value 0.71±0.01µg/mL. Compound **8e** ($IC_{50}$= 0.51 µg/ml) having 4-hydroxy substituent at ring B of the chalcone moiety has emerged as the most promising compound of this series. Compound **8g** with chloro substituent at 4-position showed $IC_{50}$ value of 0.53 µg/ml. This could suggest that certain aromatic substituents at 4-position on ring B of the chalcone moiety are important for antileishmanial activity. The significance of the 4-hydroxyl group was investigated further and compound **8e** ($IC_{50}$= 0.51 µg/ml) was selected as a representative derivative to explore the effect of cyclization. As can be seen**,** our pyrazoline derivative **8i,** with $IC_{50}$= 0.47 µg/ml, is more potent than corresponding chalcone analogue **8e**.

To determine whether the SAR study around thioxo-analogues has improved effect on the biological activity, *in vitro* antileishmanial activity was evaluated. SAR data in **Table 3** shows that the most potent compound of this series **12c** ($IC_{50}$= 0.51+0.04) has hydroxyl group at *meta* position of the C-4 phenyl ring on DHPM and at *para* position of chalcone ring B. Addition of nitro group at position $R^1$ results in decrease in activity compared to hydroxyl group.

The synthesized compounds were also tested against the promastigotes of *L. donovani*. Most of compounds have shown no inhibition. However, lead compound **8i** have shown excellent activity with $IC_{50}$= 1.5 µg/ml. Compound **12c** have shown good activity with $IC_{50}$= 5.58µg/ml. It is concluded that our lead compound **8i** is efficient enough to eradicate both visceral and topical leishmaniasis.

### *2.4. Molecular docking analysis of designed compounds*

In an attempt to gain insights and to explore the probable binding modes of synthesized compounds, molecular docking of these compounds was performed into the active site of LmajPTR1 (*Lm*PTR1, PDB 1e7w) *via* MOE docking program. We focused on the properties of pteridine reductase 1 (PTR1) as drug target for antileishmanial drug discovery. From Protein Data Bank, the available solved X-ray structures for LmajPTR1 are: 1E7W, 1W0C, 2BF7, 1E92 and 3H4V. These crystal structures are in ternary complexes with methotrexate (MTX), 7,8-dihydrobiopterin and 2,4,6-triaminoquinazoline. Selection of MTX, a folate antagonist, resistant Leshmania, has provided much information about drug resistance. Two step folate reduction mechanisms is the similar approach followed in both leishmania as well as in resistant trypanosome. Therefore, we opted 1E7W as a useful target against resistant strains of the *L. major*. Another intracellular protozoan species, L. donovani, is responsible for the most severe form of leishmaniasis i.e. visceral leishmaniasis. *L. major* and *L. donovani* enzymes share 91% sequence identity and the catalytic residues Asp181, Tyr191, Tyr194, and Lys198 are conserved; therefore, the details of the catalytic mechanism are expected to be identical between them [26-28].

Present study encompasses the synthesis and *in vitro* evaluation of racemic DHPMs derivatives as antileishmanial agents by exploiting the *in silico* predictive power. Hence, we were interested in exploring the probable binding modes of enantiomerically pure (R) and (S) DHPMs into the active site of PTR1. Molecular docking studies were carried out on both enantiomers of the synthesized DHPMs analogues. Analysis of the 2D interactions of the compounds with better $IC_{50}$ values showed a fair correlation between the docking scores and their inhibitory activity against PTR1 (**Figure 2**). Docking analysis of the compound **8a (**$IC_{50}$= 0.59 µg/mL, binding score -11.7909 Kcal/mol) is shown in **Figure 2A**. Phenyl ring at C-4 nucleus of DHPM ring formed strong π-π interactions with Phe113. Carbonyl oxygen of α,β-unsaturated ketone pointed towards Arg17. Similarly, carbonyl oxygen of the cyclic urea moiety formed a hydrogen bond with Lys198.

In order to explore the potent inhibitory activity of chalcone (**8e)** and its pyrazoline analogue (**8i),** we docked these compounds into the active site of PTR1. The binding model of compounds **8e** and **8i** is shown in **Figure 2B-C**. Key interactions stabilized both compounds, and the important contact residues for the docked ligands were Arg17, Ser111, Phe113, Met183, Gln186 and Leu188. The phenolic ring of compound **8i**, similarly to **8e,** stabilized through H-bond with Met183, Gln186 and Leu188. The distance between the hydroxyl group and these residues is shown in **Figure 2B** and **C**. In addition, these compounds are also involved in the π-π stacking interactions between the aromatic ring A of chalcone/pyrazoline and Phe113.

The docking score, binding affinity and binding energy of ligand-protein complex were also compared. Compound **8i** has the docking score -14.0053, strong binding affinity -10.463 Kcal/mol and lower binding energy -42.899 Kcal/mol. On the other hand, fitness values of interactions for compound **8e** were -12.9871, -9.236 Kcal/mol and -40.973 Kcal/mol respectively. Therefore, it is concluded that the difference of almost 2.0 Kcal/mol in the binding energy confirmed the stabilization of ligand-protein complex of **8i** as compared to **8e.** This showed a fair correlation between the predicted binding free energy values of the compounds and their inhibitory activity against PTR1 (1E7W). Superimposition of top-ranked docking conformations revealed that phenolic ring of pyrazoline moiety of **8i** undergoes a rotation of 180 degrees relative to **8e,** which alter the position of the hydroxyl group (**Figure 3**). Despite this difference in docking orientation, phenolic group of both compounds share the same binding region and a trivial (from $IC_{50}$= 0.51 to 0.47 µg/mL) increase in the potency may be anticipated due to this conformational motion.

Parallel studies on weakly active compounds, for example compound **8a** and **8h**, were also conducted. It can be noticed from Table 2 that compounds with 5-cinnamoyl core (**8a-c)** has showed decreased activity due to missing interactions. Visual inspection of docked binding pose of compound **8a** indicates that it does not share the complete space in the binding site of PTR1 and showed very few binding interactions with target (**Figure 4A**). Similarly, compound **8h** oriented in such a way that it shows only one hydrogen bond with Lys198 (**Figure 4B**). This may be explained by its improper fitting into the active site due to bulky dimethyl amino group. The observed negative fitness values of binding interactions (-8.763 and -9.106 Kcal/mol respectively) for these compounds revealed that these compounds were not tightly fitted into the active sites. This clearly demonstrates the weak activity of these compounds.

To explore how compounds of **Series 2** interacts with the active site residues, molecular docking studies of the most active compound **12 c** was carried out. The hydroxyl group (R), pointed towards Met 183 and Gln186 and acts as a hydrogen bond donor. Carbonyl oxygen of chalcone pointed towards the guanidinium group of Arg17 as hydrogen bond acceptor. Docking poses of **12c** are shown in **Figure 5.** In view of the above, we were successful in occupying the empty space in the binding site of PTR1 and the observed negative fitness values of interactions (i.e. docking score, binding affinity and binding energy) has shown a rational correlation between the docking scores and their inhibitory activity toward PTR1.

### 2.5. *In silico* ADMET predictions

It is well recognized that employing computational absorption, distribution, metabolism and excretion (ADME) predictions in combination with *in vitro* prediction (Docking studies) as early as possible in the drug discovery process helps to reduce the number of safety issues and help to improve prediction success. This early *in silico* ADME profiling, has in fact, decreased the proportion of drug candidates that fail in clinical trials for ADME reasons. Owing to the excellent *in vitro* activity, we initiated *in silico* calculations for drug-like characteristics and ADME prediction of compounds. An inspection of the data given in **Table 4** revealed that almost all compounds of **Series 1** have octanol-water partition coefficient (i.e. LogP) values ranging from 3.49 to 5.42. However, molecular hydrophobicity, calculated as LogP, is not the only

indicator of drug absorption. Aqueous solubility of a compound is also an important factor and is the direct measure of hydrophobicity of a compound [29]. **Table 4** shows the predicted values of solubility of compounds ($S_w$ in mg/ml) and it is clear that due to the low predicted values of solubility, these compounds have shown less LogPermeability. On the other hand, amphotericin B has shown the lowest LogPermeability (-11.516) and decreased logD values (less than -2.3, **Table 4**) and these decreased values of amphotericin B are key factors responsible for its availability as IV-infusions clinically. Lead compound **8i** is also predicted to be administered *via* IV-infusion to attain 100% bioavailability due to its reduced LogPermeability (-10.5468) values. However, compound **8b** can be administered orally due to its improved native solubility (0.0143 mg/mL), logP (3.49) and LogPermeability (-9.1511). Furthermore, compound **8h** and **8i** are predicted to possess enhanced solubility in the gastric environment due to their reduced logD values (-0.30 and -0.52) irrespective of curtailed native solubility of 0.0014 and 0.0038 mg/ml respectively (**Table 4**). **12a-d** (Series 2) can be utilized to be administered *via* oral administration due to improved logD to molecular weight band distributions (>50% orally bioavailable) irrespective of their low solubilities. Total polar surface area (TPSA), another biological membrane penetration indicator, was calculated for different pH values. In the blood stream (pH=7.4), a trivial increase TPSA of our lead compound **8i** (114.85 $A^2$ to 116.46 $A^2$) and amphotericin B (319.61 $A^2$ to 324.06 $A^2$) has been observed (**Figure 6**).

It was seen that some compounds like **8f**, **8h**, **12b** and **12c** violate some of the Lipinski's rule of 5 (Ro5) as obvious from **Table 4**. But this Ro5 is not the only parameter to scrutinize the fate of the drug candidate to enter the market. As referenced drug (amphotericin B) utilized in the present research also violate the MW parameter with 924.09 Da. The allowed MW for amphotericin is <300 Da according to its log logD -2.31. It is therefore, due its high molecular weight to logD distribution (less than 50% orally bioavailable), it is administered as intravenous route to overcome the oral permeability barrier which is also obvious from its low logPermeability (-11.516). Therefore, all the compounds were screened against their allowed molecular weights to logD distributions at physiological pH 7.4.

It was found that allowed molecular weight range for these compounds depicts the accurate correlations between the oral bioavailable >50% to that of calculated logPermeability of compounds. Where, compound with no Ro5 violation (8i) but still pertain less logPermeability of -10.5468, as its allowed molecular weight is between 350-400 Da. Henceforth, it pertains less oral bioavailability irrespective of obeying the Ro5 and is suited to be administered intravenously.

With respect to tissue distribution, logD value of compounds was correlated with the plasma protein binding (PPB). The logD values of all the compounds at various physiological pH of the alimentary canal is tabulated and shown in **Figure 7a-b**. From the data presented in **Figure 7**, it is significant that almost all the compounds pertaining logD values greater than 3 have more than 90% PPB, which is consistent with results described in literature [30]. However, high protein binding of amphotericin B is eccentric to its high molecular weight (i.e. greater than 500 Da) rather than logD [31]. Owing to the increased PPB capacity, lead compounds **8i, 12a-12d** pertain long duration of action and can be used to eradicate the visceral and topical leishmaniasis (**Table 4)**. Furthermore, increase in logD values of compound is responsible for

increased metabolic clearance over renal clearance as renal clearance decreases with lipophilicity [32]. In addition, renal clearance is also related with the molecular weight distribution and hydrogen bond donor (HBD) capacity of compounds. Hence, small molecules with MW below 350 Da will eliminate *via* renal and higher molecular weight compounds *via* partially fecal route [33]. Similarly, compounds with HBD >4 will have greater tendency to eliminate *via* phase-II metabolism (glucoronidation) [34]. The renal clearance of the compounds were predicted by their unbound percentage in the blood and tabulated in ml/min/kg (**Table 4).** These predicted renal clearances may vary due to molecular weight distribution, active secretion (*via* ATP driven efflux transporter P-glycoprotein). Therefore active eliminations are prone at the distal parts of nephron (**Figure 8a-c**). The literature cut off values for propensity of molecules to be the substrate at P-glycoprotein is: > 400 Da for MW and > 90 $A^2$ for TPSA [35]. These predictions are promising and hence deserve to be investigated further to assess the complete drug-likeness.

## 3. Conclusion

In summary, we have carried out medicinal chemistry-driven structure based modifications of 3,4-dihydropyrimidine core. It is clear from the SAR exploration around DHPM **8** analogues that certain aromatic substituents at 4-position on ring B of the chalcone moiety are important for antileishmanial activity. Attempt to decrease the number of rotatable bonds resulted in increased potency presumably due to hydrogen bond donor pattern of 4-OH group. In terms of potency, SAR exploration in Series 2 compounds offered generally lower potency over Series 1 compounds. In addition, *in silico* ADME data revealed that the results of both series encourage further investigation on structural optimization and on *in vivo* models.

## 4. Experimental

### *4.1 General*

All the reagents and solvents were purchased from standard commercial vendors and were used without any further purification. Sonication was performed in Elma E 30 H (Germany) ultrasonic cleaner with a frequency of 37 KHz and a nominal power of 250 W. $^{1}$H and $^{13}$C-NMR spectra were recorded in deutrated solvents on a Bruker spectrometer at 300 and 75 MHz respectively using tetramethylsilane (TMS) as internal reference. Chemical shifts are given in δ scale (ppm). Melting points were determined in open capillaries using Gallenkamp melting point apparatus (MP-D). The progress of all the reactions was monitored by TLC on 2.0 x 5.0 cm aluminum sheets pre-coated with silica gel 60F254 with a layer thickness of 0.25 mm (Merck). LC-MS spectra were obtained using Agilent technologies 1200 series high performance liquid chromatography comprising of G1315 DAD (diode array detector) and ion trap LCMS G2445D SL.

**4.2. General method for the synthesis of 3,4-dihydropyrimidine-2-ones and 3,4-dihydropyrimidine-2-thiones (1-13)**

Dihydropyrimidines were synthesized according to our previous report procedure using ultrasonication [14].

A mixture of an aldehyde (10 mmol), a diamino compound (12 mmol), a dicarbonyl compound (10 mmol, mL), $SnCl_2.2H_2O$ (10 mol %) and acetonitrile (10 mL) was mixed in a pyrex tube. The mixture was then irradiated in ultrasonic bath at 70-75$^o$C. The reaction was monitored by TLC. After the completion of the reaction, the resulting precipitate was filtered and crude product was recrystallized from an appropriate solvent or purified through column chromatography. Spectroscopic data was consistent with the previously reported for these compounds.

**4.3. Synthesis of chalcones from dihydropyrimidines (Scheme 2, 8a-8c)**

In a pyrex tube 25 mL ethanol and 30 mL of NaOH (4M) solution was added. The flask was cooled in an ice-bath and then 2 mmol DHPM (0.488 gm) and substituted aldehydes (2 mmol) was finally added and placed in ultrasonic bath at 40-50 ºC. After completion of the reaction (TLC), quenched in ice-cold water and then acidified with aq. HCl (1N). The precipitate obtained was re-crystallized from mixture of ethanol/water (1:0.5).

***4.3.1. 5-cinnamoyl-1,6-dimethyl-4-(3-nitrophenyl)-3,4-dihydropyrimidin-2(1H)-one (8a)***

Yield 610 mg (81%). Brown solid; Mp. 219-221 ºC. $R_f$=0.45 (n-hexane/ethyl acetate 3:1). $^1$H NMR (300 MHz, DMSO-$d_6$): 8.81 (br s, 1H, NH), 8.19 (m, 2H, Ar-H), 7.92 (d, 1H, *J* = 15.6 Hz, *H*-$C_\beta$), 7.68 (m, 2H, Ar-H), 7.41 (d, 1H, *J* = 15.6 Hz, *H*-$C_\alpha$), 7.10 (m, 5H, Ar-H), 5.11 (d, 1H, *J* = 3.0 Hz, C*H*), 3.19 (s, 3H, N-$CH_3$), 2.15 (s, 3H, $CH_3$). $^{13}$C-NMR (75 MHz, DMSO-): 190.1, 152.7, 151.0, 150.20, 149.0, 147.1, 144.3, 136.4, 134.9. 132.6, 130.3, 129.9, 129.1, 126.2, 125.3, 120.0, 54.1, 30.7, 18.1. MS (EI) m/z 377.0 $[M]^+$.

***4.3.2. (E)-5-cinnamoyl-4-(4-hydroxyphenyl)-1,6-dimethyl-3,4-dihydropyrimidin-2(1H)-one (8b)***

Yield 536 mg (77%). Yellow solid. Mp. 199-200ºC. $R_f$=0.41 (n-hexane/ethyl acetate 5:1);$^1$H NMR (300 MHz, DMSO-d6): δ 9.3 (s, 1H, OH), 8.87 (br s, 1H, NH), 7.81 (d, *J* = 15.9 Hz, 1H, H-$C_\beta$), 7.67 (d, *J* = 15.9 Hz, 1H, H-$C_\alpha$), 7.14 (m, 7H, Ar-*H*), 6.83 (d, 2H, , *J* = 6.6 Hz, Ar-*H*), 5.07 (d, 1H, *J* = 3.3 Hz, C*H*), 3.17 (s, 3H, N-$CH_3$), 2.18 (s, 3H, $CH_3$); $^{13}$C-NMR (75 MHz, DMSO-): δ 190.0, 162.2, 157.9, 153.1, 152.0, 149.4, 145.1, 129.8, 128.4, 128.2, 122.0, 120.7, 118.0, 115.0, 54.9, 30.6, 18.0. MS (EI) m/z 348.0 [M]+.

***4.3.3. (E)-4-(4-chlorophenyl)-5-cinnamoyl-1,6-dimethyl-3,4-dihydropyrimidin-2(1H)-one (8c)***

Yield 651 mg (89%). Yellow solid. Mp. 211-212 ºC. $R_f$: 0.47 (n-hexane/ethyl acetate 2:1). $^1$H NMR (300 MHz, DMSO-d6): δ 8.93 (br s, 1H, NH), 7.79 (d, 1H, *J* = 15.9 Hz, H-$C_\beta$), 7.59 (d, 1H, *J* = 15.9 Hz, H-$C_\alpha$), 7.43 (d, 1H, *J* = 8.4 Hz, Ar-*H*), 7.32 (d, 1H, *J* = 8.4 Hz, Ar-*H*), 7.14 (m, 5H, Ar-*H*), 5.13 (d, 1H, *J* = 3.3 Hz, C*H*), 3.21 (s, 3H, N-$CH_3$), 2.23 (s, 3H, $CH_3$); $^{13}$C-NMR (75 MHz, DMSO-): δ 192.6, 152.4, 150.9, 145.7, 135.3, 130.2, 128.32, 127.1, 125.2, 122.9, 121.1, 119.8, 55.1, 30.3, 17.8. MS (EI) m/z 366.0 [M]+.

**4.4. Synthesis of 4′-aminochalcones (Scheme 3a, 14-18)**

4′-aminochalcones were synthesized according to literature procedure [36].

To a stirred ice-cold solution of 4'-aminoacetophenone (1.352 gm, 10 mmol) and potassium hydroxide (1-2 pellets) in 20 mL ethanol was added drop-wise substituted aromatic benzaldehydes (10 mmol). Temperature of the reaction mixture was kept at room temperature. After completion of reaction mixture was poured into ice-water with continuous stirring and kept at 0-4 $^{o}$C overnight. The precipitate obtained was filtered, washed and re-crystallized from mixture of ethanol/water (1:0.5).

***4.4.1. (E)-1-(4′-aminophenyl)-3-phenylprop-2-en-1-one (14)***

**14** was synthesized by using 4'-aminoacetophenone (1.352 gm, 10 mmol) and benzaldehyde (1.06 gm, 10 mmol). Yellow solid; Yield 1.54 gm (69%). Mp = 146 ºC; $R_f$ =0.51 (n-hexane:ethyl acetate 3:1);. $^1$H NMR (300 MHz, $CDCl_3$): δ (ppm) = 7.97 (d, J = 15.9 Hz, 1H, H-$C_\beta$), 7.69 (m, 3H, H-$C_\alpha$, 2 × Ar-*H*), 7.18-7.30 (m, 5H, Ar-*H*), 6.81 (m, 2H, Ar-H), 5.82 (bs, 2H, $NH_2$),; EIMS: $C_{15}H_{13}NO$, 223.0.

***4.4.2. (E)-1-(4′-aminophenyl)-3-(4-hydroxyphenyl)prop-2-en-1-one (15)***

**15** was synthesized by using 4'-aminoacetophenone (1.352 gm, 10 mM) and 4-hydroxyphenyl benzaldehyde (1.22 gm, 10 mM). Yellow solid. Yield. 1.67 gm (71%). $R_f$ =0.55 (n-hexane:ethyl acetate 3:1). $^1$H NMR (300 MHz, $CDCl_3$): δ 9.71 (s, 1H, OH), 7.93 (d, *J* = 15.6 Hz, 1H, H-$C_\beta$), 7.65 (m, 3H, H-$C_\alpha$, 2 × Ar-*H*), 7.27-7.29 (m, 2H, Ar-*H*), 6.79-6.83 (m, 4H, Ar-*H*), 5.87 (bs, 2H, $NH_2$); MS (EI) m/z 239.0 [M]+.

***4.4.3. (E)-1-(4′-aminophenyl)-3-(4-nitrophenyl)prop-2-en-1-one (16)***

**16** was synthesized by using 4'-aminoacetophenone (1.352 gm, 10 mM) and 4-nitrophenyl benzaldehyde (1.51 gm, 10 mM). Dark yellow solid, Yield. 1.53 gm (57%). $R_f$ =0.40 (n-hexane/ethyl acetate 3:1). Mp: 185 ºC.; $^1$H NMR (300 MHz, $CDCl_3$) δ 8.21 (m, 2H, Ar-H), 7.98 (d, *J* = 15.6 Hz, 1H, H-$C_\beta$), 7.71 (d, *J* = 15.6 Hz, 1H, H-$C_\alpha$), 7.61 (m, 4H, Ar-*H*), 6.81 (m, 2H, Ar-H), 5.81 (bs, 2H, $NH_2$); LC-MS m/z 269 [M+H].

***4.4.4. (E)-1-(4′-aminophenyl)-3-(4-chlorophenyl)prop-2-en-1-one (17)***

**17** was synthesized by using 4'-aminoacetophenone (1.352 gm, 10 mM) and 4-chlorophenyl benzaldehyde (1.40 gm, 10 mM). Yellow solid, Yield 1.31 gm (51%). $R_f$ =0.53 (n-hexane/ethyl acetate 2:1). Mp: 171 ºC.; $^1$H NMR (300 MHz, $CDCl_3$) δ 7.93 (d, *J* = 15.9 Hz, 1H, H-$C_\beta$), 7.69 (m, 3H, H-$C_\alpha$, 2 × Ar-*H*), 7.23-7.25 (m, 4H, Ar-*H*), 6.86-6.88 (m, 2H, Ar-*H*), 5.83 (bs, 2H, $NH_2$); LC-MS m/z 258 [M+H].

***4.4.5. (E)-1-(4′-aminophenyl)-3-(4-(dimethylamino)phenyl)prop-2-en-1-one (18)***

**18** was synthesized by using 4'-aminoacetophenone (1.352 gm, 10 mM) and 4-(dimethylamino)phenyl benzaldehyde (1.492 gm, 10 mM). Light yellow solid, Yield. 81%. $R_f$ =0.47 (n-hexane/ethyl acetate 3:1). m.p =157 ºC; $^1$H NMR (300 MHz, $CDCl_3$) δ 7.93 (d, *J* = 15.6 Hz, 1H, H-$C_\beta$), 7.61 (m, 3H, H-$C_\alpha$, 2 × Ar-*H*), 7.23-7.27 (m, 2H, Ar-*H*), 6.73-6.77 (m, 4H, Ar-*H*), 5.86 (bs, 2H, $NH_2$), 2.97 (s, 6H, $N(CH_3)_2$) ; LC-MS m/z 267 [M+H].

**4.5. Synthesis of 6-bromo DHPM (Scheme 3b)**

Dihydropyrimidine (**8**) (2.44 gm, 10 mmol) was suspended in 30 mL $CHC1_3$ and then bromine (0.52 ml, 10 mmol) was added drop-wise through dropping funnel and stirred at 4 ºC for 18 hrs. After completion of reaction, the solvent was removed under reduced pressure and residue was purified by silica gel column chromatography to afford the product.

**4.5.1. 5-acetyl-6-(bromomethyl)-1-methyl-4-phenyl-3,4-dihydropyrimidin-2(1H)-one (19A)**

Yield. 2.51 gm (78%). White solid. Mp: 135-137 ºC. $R_f$ : 0.38 (n-hexane:ethyl acetate 3:1). UV absorption at 297.00 nm, $^1$H NMR (300 MHz, DMSO-$d_6$): δ 9.49 (s,1H, *NH*), 7.24 (m, 5H, Ar-H), 5.16 (d, 1H, *J*=3.0 Hz, *CH*), 4.64 (s, 2H, $CH_2$Br), 3.16 (s, 3H, N-$CH_3$), 2.50 (s, 3H, CO$CH_3$). $^{13}$C-NMR (75 MHz, DMSO-$d_6$): δ 194.7, 152.9, 145.9, 120.2-127.0, 101.18, 53.3, 39.78, 30.5, 29.4; LC-MS m/z 323 (M+H).

**4.5.2. 5-(2-bromoacetyl)-1,6-dimethyl-4-phenyl-3,4-dihydropyrimidin-2(1H)-one (19B)**

Yield. 0.58 gm (18%). White solid. LC-MS m/z 323 (M+H)

**4.6. C-6 substitution reaction of brominated DHPM (Scheme 3b, 8d-h)**

In a pyrex tube, a mixture of 4′-aminochalcones (**14-18**, 2 mmol) and 6-bromo DHPM (0.646 gm, 2 mmol) in THF (5 mL) was heated in ultrasonic bath at 40 ºC. The reaction was monitored by TLC. The precipitate obtained was filtered, washed with sodium bicarbonate (2 × 10 mL, 0.1M). The crude solid was recrystallized from a mixture of petroleum ether/ethanol (1:1).

***4.6.1.(E)-5-acetyl-6-((4-cinnamoylphenylamino)methyl)-1-methyl-4-phenyl-3,4-dihydropyrimidin-2(1H)-one (8d)***

Yellow crystals. Yield 716 mg (77%). LC-MS purity 99.98%, $t_R$= 5.3min. Mp.=211-213 ºC. $R_f$ =0.53 (n-hexane/ethyl acetate 3:1). $^1$H NMR (300 MHz, DMSO-$d_6$) δ 9.53 (s,1H, NH pyrimidine), 7.83 (d, *J* = 15.9 Hz, 1H, H-$_\beta$ (Vinyl)), 7.71 (m, 3H, H-$C_\alpha$ 2 × Ar-*H*), 7.11 (m, 10H, Ar-*H*), 6..71 (d, 2H, Ar-*H*), 6.07 (t, 1H, *J*=5.7Hz, 1H , $CH_2$-*NH*), 5.17 (d, 1H, *J*=3.0 Hz, CH), 3.23 (s, 3H, N-$CH_3$), 3.13 (d, 2H, *J*=7.2 Hz, $CH_2$N), 2.31 (s, 3H, CO$CH_3$); $^{13}$C-NMR (75 MHz, DMSO-d6): δ 195.0, 190.0, 151.1, 147.3, 142.5, 133, 120.0-129.0, 103.6, 59.33, 53.3, 30.1, 28.7. LC-MS m/z 466.2 [M+H].

***4.6.2. (E)-5-acetyl-6-((4-(3-(4-hydroxyphenyl)acryloyl)phenylamino)methyl)-1-methyl-4-phenyl-3,4-dihydro-pyrimidin-2(1H)-one (8e)***

Yellow crystals. Yield. 548 mg (57%). Yield 716 mg (77%). LC-MS purity 100.00%, $t_R$= 4.9 min. Mp: 223-224 ºC. $R_f$: 0.42 (n-hexane/ethyl acetate 5:1). $^1$H NMR (300 MHz, DMSO-$d_6$) δ 9.71 (s, 1H, OH), 9.57 (br s, 1H, NH pyrimidine), 7.79 (d, 1H, *J* = 15.9 Hz, $H_\beta$ (Vinyl)), 7.63 (m, 3H, 1H-$C_\alpha$, 2 × Ar-*H*), 7.13 (m, 7H, Ar-*H*), 6.79 (m, 4H, Ar-H), 6.13 (t, 1H, *J*=5.7 Hz, $CH_2$-*NH*), 5.21 (d, 1H, *J*=3.0 Hz, CH), 3.25 (s, 3H, N-C$H_3$), 3.11 (d, 2H, *J*=7.2 Hz, $CH_2$N), 2.37 (s, 3H, CO$CH_3$). $^{13}$C-NMR (75 MHz, DMSO-d6): δ 195.0, 190.5, 159.1, 150.2, 147.6, 142.7, 133.9, 131.0, 130.5, 129.5, 129.2, 128.1, 127.5, 118.9, 113.5, 103.3, 58.9, 52.1, 30.4, 28.1. LC-MS m/z 482.2 [M+H].

***4.6.3. (E)-5-acetyl-1-methyl-6-((4-(3-(3-nitrophenyl)acryloyl)phenylamino)methyl)-4-phenyl-3,4-dihydropyrimidin-2(1H)-one (8f)***

Brown crystals. Yield 643mg (63%). LC-MS purity 100.00%, $t_R$=6.0 min. Mp: 229-231 ºC. $R_f$: 0.42 (n-hexane/ethyl acetate 3:1). $^1$H NMR (300 MHz, DMSO-$d_6$) δ 9.61 (br s, 1H, NH pyrimidine), 8.37 (s, 1H, Ar-H), 8.17 (m, 1H, Ar-H), 7.98 (d, 1H, *J* = 15.9 Hz, $H_\beta$ (Vinyl)), 7.71 (d, 1H, *J* = 15.9 Hz, H-$C_\alpha$), 7.51 (m, 4H, Ar-*H*), 7.14 (m, 5H, Ar-H), 6.73 (d, 2H, Ar-H), 6.19 (t, 1H, *J*=5.7 Hz, $CH_2$-*NH*), 5.17 (d, 1H, *J*=3.0 Hz, C*H*), 3.29 (s, 3H, N-$CH_3$), 3.13 (d, 2H, J=7.2 Hz, $CH_2$N), 2.33 (s, 3H, CO$CH_3$). $^{13}$C-NMR (75 MHz, DMSO-$d_6$): δ 195.5, 189.1, 150.5, 149.0, 147.6, 142.3, 121.9, 113.8-132.0, 103.2, 58.7, 53.6, 30.9, 27.9. LC-MS m/z 511.2 [M+H].

***4.6.4. (E)-5-acetyl-6-((4-(3-(4-chlorophenyl)acryloyl)phenylamino)methyl)-1-methyl-4-phenyl-3,4-dihydro-pyrimidin-2(1H)-one (8g)***

Yellow crystals. Yield. 509 mg (51%). LC-MS purity 99.53%, $t_R$=8.9 min. Mp: 193-194 ºC. $R_f$: 0.50 (n-hexane/ethyl acetate 2:1). $^1$H NMR (300 MHz, DMSO-$d_6$) δ 9.58 (bs, 1H, NH pyrimidine), 7.91 (d, 1H, *J* = 15.9 Hz, $H_\beta$ (Vinyl)), 7.67 (m, 3H, H-$C_\alpha$, 2 × Ar-*H*), 7.10 (m, 9H, Ar-*H*), 6.79 (m, 2H, Ar-*H*), 6.27 (t, 1H, *J*=5.7Hz, 1NH , $CH_2$-*NH*), 5.29 (d, 1H, *J*=3.0 Hz, C*H*), 3.37 (d, 2H, J=7.2 Hz, $CH_2$N), 3.21 (s, 3H, N-$CH_3$), 2.37 (s, 3H, CO$CH_3$); $^{13}$C-NMR (75 MHz, DMSO-d6): δ 195.5, 189.3, 159.6, 152.6, 151.1, 146.9, 144.3, 142.4, 135.2, 134.1, 130.0, 127.9, 126.6, 125.6, 123.0, 120.3, 119.9, 102.9, 58.3, 53.8, 30.3, 27.3. LC-MS m/z 500.2 [M+H].

***4.6.5. (E)-5-acetyl-6-((4-(3-(4-(dimethylamino)phenyl)acryloyl)phenylamino)methyl)-1-methyl-4-phenyl-3,4-dihydropyrimidin-2(1H)-one (8h)***

Brown solid. Yield 742 mg (73%). LC-MS purity 100.00%, $t_R$=10.2 min. Mp: 237-239 ºC. $R_f$ =0.45 (n-hexane/ethyl acetate 3:1). $^1$H NMR (300 MHz, DMSO-$d_6$) δ 9.60 (br s, 1H, NH pyrimidine), 7.99 (d, 1H, *J* = 15.9 Hz, H-$_\beta$), 7.65 (m, 3H, H-$C_\alpha$, 2 × Ar-*H*), 7.06 (m, 7H, Ar-*H*), 6.68 (m, 4H, Ar-*H*), 6.26 (t, 1H, *J*=5.7Hz, $CH_2$-*NH*), 5.28 (d, 1H, *J*=3.0 Hz, C*H*), 3.37 (d, 2H, *J*=7.2 Hz, $CH_2$N), 3.20 (s, 3H, N-$CH_3$), 2.91 (s, 6H, N($CH_3$)$_2$), 2.33 (s, 3H, CO$CH_3$). $^{13}$C-NMR (75 MHz, DMSO-$d_6$): δ 195.0, 189.6, 151.4, 154.9, 151.4, 149.4, 146.5, 142.3, 132.0, 130.6, 129.6, 128.8, 128.5, 127.2, 126.5, 124.5, 122.2, 121.3, 120.2, 102.4, 58.0, 53.2, 41.4, 30.8, 27.0; LC-MS m/z 509.2 [M+H].

**4.7. Synthesis of pyrazolines (Scheme 4, 8i)**

In a pyrex tube containing 2.5 mmol of solid NaOH in ethanol (15 mL) was added chalcone (2 mmol) and hydrazine (2 mmol). The reaction mixture was heated in ultrasonic bath at 40 ºC. Upon completion of the reaction (TLC), the reaction mixture was cooled to room temperature and quenched with 5 mL of a solution of dil. HCl. The reaction mixture concentrated to dryness in vacuum to afford the product as a solid. The crude solid was recrystallized from a mixture of n-hexane and methanol.

***4.7.1. 5-acetyl-6-((4-(5-(4-hydroxyphenyl)-4,5-dihydro-1H-pyrazol-3-yl)phenylamino)methyl)-1-methyl-4-phenyl-3,4-dihydropyrimidin-2(1H)-one (8i)***

Pale yellow solid. Yield 502 mg (51%). LC-MS purity 100.00%, $t_R$=3.3 min. Mp: 198-200 ºC. $R_f$ =0.47 (n-hexane/ethyl acetate 3:1). $^1$H NMR (300 MHz, DMSO-$d_6$) δ 9.87 (s,1H, pyrimidine-NH), 9.10 (s, 1H, Ar-

OH), 8.80 (s,1H, pyrazoline-NH), 7.79 (d, 2H, *J*=7.5 Hz, Ar-*H*), 6.98 (m, 7H, Ar-*H*), 6.64 (d, 2H, *J*=8.4 Hz, Ar-*H*), 6.42 (d, 2H, *J*=8.4 Hz, Ar-H), 5.99 (t, 1H, *J*=5.7 Hz, $CH_2$-*NH*), 5.15 (d, 1H, *J*=3.0 Hz, pyrimidine-CH), 4.81 (dd, J=12.3 Hz, 7.8 Hz, 1H, pyrazoline-CH), 3.93 (dd, *J*=17.1 Hz, 12.3 Hz, 1H, pyrazoline-CH), 3.44 (dd, *J*=7.8 Hz, 17.1 Hz, 1H, pyrazoline-CH), 3.23 (s, 3H, N-$CH_3$), 3.16 (d, 2H, *J*=7.2 Hz, $CH_2$N), 2.39 (s, 3H, CO$CH_3$); $^{13}$C-NMR (75 MHz, DMSO-d6): δ 195.0, 159.95, 153.50, 151.1, 149.9, 148.9, 142.5, 139.0, 128.9, 128.8, 127. 9, 126.6, 124.9, 123.5, 121.1, 121.0, 120.0, 103.0, 76.0, 59.33, 56.0, 51.0, 30.5, 28.1; LC-MS m/z 493.2 [M+H].

**4.8. Series 2: SAR exploration around thioxo-analogues 12 and 13 (12a-d).**

In a pyrex tube, a mixture of 4′-aminochalcones (2 mmol) and thioxo DHPM **12** (0.58 gm, 2 mmol) and **13** (0.585 gm, 2 mmol) in THF (5 mL) was heated in ultrasonic bath at 40 ºC. The reaction was monitored by TLC. The precipitate obtained was filtered, washed with sodium bicarbonate (2 × 10 mL, 0.1M). The crude solid was recrystallized from a mixture of petroleum ether/ethanol (1:1).

***4.8.1. (E)-N-(4-(3-(4-hydroxyphenyl)acryloyl)phenyl)-6-methyl-2-thioxo-4-p-tolyl-,3,4-dihydropyrimidine -5-carboxamide (12a)***

Yellow crystals. Yield 589 mg (61%). LC-MS purity 99.98%, $t_R$=17.6 min. Mp: 219-221 ºC. $R_f$ =0.38 (n-hexane/ethyl acetate 5:1). $^1$H NMR (300 MHz, DMSO-$d_6$) δ 9.88 (s, 1H, OH), 9.57 (br s,1H, NH pyrimidine), 9.23 (br s, 1H, N*H*-CO), 8.24 (br s, 1H, NH), 8.04 (d, 1H, *J* = 15.6 Hz, $H_\beta$ (Vinyl)), 7.71 (m, 4H, Ar-H), 7.59 (d, 1H, *J* = 15.6 Hz, H-$C_\alpha$), 7.21 (m, 2H, Ar-*H*), 7.01 (m, 4H, Ar-H), 6.79 (m, 2H, Ar-H), 5.14 (d, 1H, *J*=3.3 Hz, CH), 2.21 (s, 6H, 2×$CH_3$); $^{13}$C-NMR (75 MHz, DMSO-d6): δ 190.5, 182.8, 167.2, 159.6, 148.5, 144.7, 142.3, 139.9, 135.3, 133.5, 131.6, 129.8, 129.2, 129.0, 128.9, 128.8, 127.0, 125.6, 124.9, 113.0, 100.72, 54.6, 26.3, 18.2. LC-MS m/z 484.2 [M+H].

***4.8.2. (E)-6-methyl-N-(4-(3-(3-nitrophenyl)acryloyl)phenyl)-2-thioxo-4-p-tolyl-3,4-dihydropyrimidine-5-carboxamide (12b)***

Dark yellow crystals. Yield 584 mg (57%). LC-MS purity 100.00%, $t_R$=11.2 min. Mp =242-243 ºC. $R_f$ =0.38 (n-hexane/ethyl acetate 5:1). $^1$H NMR (300 MHz, DMSO-$d_6$) δ 9.59 (bs,1H, NH pyrimidine), 9.27 (br s, 1H, N*H*-CO), 8.50 (s, 1H, Ar-H), 8.37 (br s, 1H, NH), 8.29 (m, 1H, Ar-H), 8.17 (d, 1H, *J* = 15.9 Hz, $H_\beta$), 7.99 (d, 1H, *J* = 15.9 Hz, $H_\alpha$), 7.82 (d, 4H, Ar-H), 7.67 (d, 1H, Ar-H), 7.65 (d, 1H, Ar-H), 7.14 (s, 4H, Ar-H), 5.17 (d, 1H, *J*=3.3 Hz, CH), 2.23 (s, 6H, 2×$CH_3$); $^{13}$C-NMR (75 MHz, DMSO-$d_6$): δ 190.5, 182.8, 167.2, 151.0, 148.5, 144.7, 124.9, 113.0-132.0, 54.6, 26.3, 18.2. LC-MS m/z 513.2 [M+H].

***4.8.3. (E)-4-(3-hydroxyphenyl)-N-(4-(3-(4-hydroxyphenyl)acryloyl)phenyl)-6-methyl-2-thioxo-3,4-dihydro-pyrimidine-5-carboxamide (12c)***

Yellow crystals. Yield 650 mg (67%). LC-MS purity 100.00%, $t_R$=10.3 min. Mp: 219-221 ºC. $R_f$ =0.51 (Chloroform/Methanol 5:1). $^1$H NMR (300 MHz, DMSO-$d_6$) δ 9.96 (br s, 1H, O*H*-pyrimidine ) 9.68 (s, 1H, O*H*-chalcone), 9.47 (bs,1H, NH-pyrimidine), 9.21 (br s, 1H, N*H*-CO), 8.14 (br s, 1H, NH-pyrimidine), 7.99 (d, 1H, *J* = 15.9 Hz, $H_\beta$), 7.61 (m, 5H, H-$C_\alpha$, 4×Ar-*H*), 7.23 (d, 2H, *J* = 6.3 Hz, Ar-*H*), 6.96 (t, 1H, *J* = 8.1 Hz, Ar-H), 6.74 (m, 3H, *J* = 5.1 Hz, Ar-H), 6.71 (d, 2H, *J* = 5.1 Hz, Ar-H), 5.27 (d, 1H, *J*=3.3 Hz, CH), 2.26 (s, 3H, $CH_3$); $^{13}$C-NMR (75 MHz, DMSO-$d_6$): δ 191.8, 182.1, 167.6, 160.4, 155.9, 148.7, 145.1,

144.9, 142.3, 131.1, 130.2, 129.6, 129.4, 128.7, 125.5, 124.1, 123.2, 120.1, 115.2, 112.0, 100.2, 54.9, 18.6. LC-MS 486.1 [M+H].

***4.8.4. (E)-4-(3-hydroxyphenyl)-6-methyl-N-(4-(3-(3-nitrophenyl)acryloyl)phenyl)-2-thioxo-3,4-dihydro pyrimidine-5-carboxamide (12d)***

Yellow crystals. Yield 648 mg (63%). LC-MS purity 100.00%, $t_R$=11.9 min. Mp: 229-230 ºC. $R_f$ =0.57 (Chloroform/Methanol 3:1). $^1$H NMR (300 MHz, DMSO-$d_6$) δ 9.83 (br s, 1H, O*H*-pyrimidine ), 9.51 (bs, 1H, NH-pyrimidine), 9.23 (br s, 1H, N*H*-CO), 8.59 (s, 1H, Ar-H), 8.43 (br s, 1H, NH-pyrimidine), 8.29 (m, 1H, Ar-H), 8.18 (d, 1H, *J* = 15.9 Hz, $H_\beta$), 7.94 (d, 1H, *J* = 15.9 Hz, H-$C_\alpha$), 7.85 (d, 4H, *J* = 6.6 Hz, Ar-H), 7.63 (d, 1H, *J* = 6.3 Hz, Ar-H), 7.49 (m, 1H, Ar-H), 7.011 (m, 1H, Ar-H), 6.67 (m, 3H, Ar-H), 5.27 (d, 1H, *J*=3.3 Hz, CH), 2.26 (s, 3H, $CH_3$); $^{13}$C-NMR (75 MHz, DMSO-$d_6$): δ 191.2 (C=O), 181.3 (C=S), 167.1 (NH*C*=O), 161.9 (*C*-OH-pyrimidine), 151.8 (C-$NO_2$), 148.3 ($C_\beta$), 145.0 ($CH_3$C=C), 124.1 ($C_\alpha$), 113.3-129.2 (*C*-aromatic), 54.7 (*C*H-Ar), 26.2 (C-aromatic-$CH_3$), 18.5 ($CH_3$); LC-MS m/z 515.1 [M+H].

**4.8. Computational studies**

***3.8.1. Docking studies***

Docking studies were performed, using the Molecular Operating Environment (MOE) version 2011.12. The program operated under 'Windows XP' operating system. To initialize the *in silico* studies, high resolution crystal structures of proteins were retrieved from the PDB (PDB ID 1E7W, from L. major). The 3D protonation of the 1E7W was done and energy minimization of the retrieved protein molecule was carried out by using default parameters of MOE energy minimization algorithm [gradient: 0.05, Force Field: MMFF94X]. Root mean square deviation (RMSD) was used to compare the ligand between the predicted and its corresponding crystal structure. The resulting docked poses with RMSD less than 1.5Å were clustered together. The lowest energy minimized pose was used for further analysis.

***4.8.2. ADMET predictions***

Various descriptors like logP, solubility (Sw) calculated as logS by MOE software and converted to mg/ml units. Hydrogen bond acceptor (HBA), hydrogen bond donor (HBD), number of rotatable bonds (NOR) and molecular weight (MW) were calculated by MOE software. While, logD7.4 and total polar surface area (TPSA) was calculated via Marvin 6.0.0 software of Chemaxon [37]. Whereas, renal clearance (Cl), plasma protein binding (PPB) and LogPermeability were calculated theoretically [38].

**4.9. *In vitro* antileishmanial activity**

Antileishmanial activity of the compounds was assayed using a pre-established culture of clinical isolate of *L. major* and *L. donovani* obtained from National Institute of Health (NIH), Islamabad, Pakistan [10, 18]. Promastigotes were cultured in medium 199 (Cassion Laboratories, Inc. USA) containing 10 % fetal bovine serum (ICN Flow, UK), HEPES (4-(2-hydroxyethyl)-1-piperazineethanesulfonic acid), sodium bicarbonate (Sigma), penicillin (ICN Biochemicals, Inc. Germany), and streptomycin (Sigma). Incubation and growth of the parasite were carried out at 24 $^o$C. Briefly after 6–7 days of the culture, the promastigotes were

centrifuged at 3,000 rpm for 3 min, the supernatant was discarded and the pellet was washed three times with phosphate buffer saline (MP-Biomedicals, Inc. France) and re-suspended in medium 199 at 2 9 10 6 cell/mL. Promastigotes were seeded in 96-well round bottom microtiter plates (TPP, Switzerland) containing serial dilution of the compound and media 199. Amphotericin B (BioChemica, Germany) and DMSO were used as positive and negative controls, respectively. The plates were incubated for 72 h at 24 $^{o}$C in shaker incubator. All the compounds were assayed in triplicate and the number of alive parasites was determined by counting in Neubauer chamber. The inhibitory concentrations for the 50 % of the inhibition IC were calculated by GraphPad Prism (GraphPad Prism Software, Inc. USA) software and data reported as the mean ± SD.

**Acknowledgments**

The Higher Education Commission (HEC), Pakistan is thankfully acknowledged for providing financial support to Umer Rashid for its startup grant under IPFP program (HEC No: PM-IPFP/HRD/HEC/2011/346). The authors are also thankful to Chemistry Department, Quaid-i-Azam University and National Institute of Health (NIH), Islamabad, Pakistan for providing facilities.

**References**

[1] K.R. Killick, The biology and control of phlebotomine sand flies. Clin. Dermatol. 17 (1997) 279-289.

[2] S. N Advait., K. Shilpi, B. K. Arun, S. Frantisek, B. Andriy, J. N. M. Casey, K. C. Naveen, P. Nagendar, S. B. Frederick, H. G. Michael, M. Valentina, Recent Developments in Drug Discovery for Leishmaniasis and Human African Trypanosomiasis. Chem. Rev., 114 (2014), 11305–11347.

[3] J. N. Sangshetti, F. A. K. Khan, A. A. Kulkarni, R. Arote, R.H. Patil, Antileishmanial drug discovery: comprehensive review of the last 10 years. RSC Adv. 5 (2015) 32376- 32415.

[4] S. Sundar, M. Chatterjee, Visceral Leishmaniasis-Current Therapeutic Modalities. Ind. J. Medical Res. 123 (2006) 345-352.

[5] M. M. Salem, K.A. Werbovetz, Natural products from plants as drug candidates and lead compounds against leishmaniasis and trypanosomiasis. Curr. Med. Chem. 13 (2006) 2571-2598.

[6] S. Gannavaram, R. Dey, K. Avishek, A. Selvapandiyan, P. Salotra, H. L. Nakhasi, Biomarkers of vaccine-induced immunity. Front. Immunol. 5 (2014), 241–249.

[7] J.M. Mutiso, J.C. Macharia, M.N. Kiio, J.M. Ichagichu, H. Rikoi, M.M. Gicheru, Development of Leishmania vaccines: predicting the future from past and present experience. J Biomed Res. 27 (2013) 85-102.

[8] D. M. Claborn, The biology and control of Leishmaniasis vectors. J. Glob. Infec. Dis. 2 (2010) 127-134.

[9] A. Foroumadi, S. Emami, M. Sorkhi, M. Nakhjiri, Z. Nazarian, S.Heydari, S. K. Ardestani, F. Poorrajab, A. Shafiee, Chromene-Based Synthetic Chalcones as Potent Antileishmanial Agents: Synthesis and Biological Activity. Chem. Biol. Drug Des. 75 (2010) 590–596.

[10] T. Narender, G. S. Shweta, A convenient and biogenetic type synthesis of few naturally occurring chromeno dihydrochalcones and their in vitro antileishmanial activity. Bioorg. Med. Chem. Lett.14 (2004) 3913–3916.

[11] N. Singh, New drug targets in Leishmania. In: Raghunath D, Nayak R, eds, Trends and Research in Leishmaniasis with Particular Reference to Kala azar. Sir Dorabji Tata Symposium Series 5 (2005) 343–363.

[12] P. Kumar, A. Kumar, S. S. Verma, N. Dwivedi, N. Singh, M. I. Siddiqi, R. P. Tripathi, A. Dube, N. Singh, Leishmania donovani pteridine reductase 1: biochemical properties and structure-modeling studies. Exp Parasitol. 120 (2008) 73–79.

[13] J. Kaur, S. Sundar, N. J. Singh, Molecular docking, structure – activity relation-ship and biological evaluation of the anticancer drug monastrol as a pteridine re-ductase inhibitor in a clinical isolate of Leishmania donovani. J. Antimicrob. Chemother. 65 (2010) 1742-1748.

[14] U. Rashid, I. Batool, A. Wadood, A. Khan,; Z. Ul-Haq, M. I. Chaudhary, F. L. Ansari, Structure based virtual screening-driven identification of monastrol as a potent urease inhibitor. J. Mol. Graphics Modell. 43 (2013) 47-57.

[15] S. F. Hassan, U. Rashid, F. L. Ansari, Z. Ul-Haq, Bioisosteric approach in designing new monastrol derivatives: An investigation on their ADMET prediction using in silico derived parameters. J. Mol. Graphics Modell. 45 (2013) 202-210.

[16] S. Kalsoom, U. Rashid, M. A. Mesaik, O. M. Abdalla, K. Hussain, W. Khan, A. Shaukat, F. Iftikhar, M. B. Khan, Z. Ul-Haq, F. L. Ansari, In vitro and in silico exploration of IL-2 inhibition of small organic molecules. Med. Chem. Res. 22 (2013) 5739-5751.

[17] G.S. Singh, Y.M. Al-Kahraman, D. Mpadi, M. Yasinzai, Synthesis of N-(1-methyl-1H-indol-3-yl)methyleneamines and 3,3-diaryl-4-(1-methyl-1H-indol-3-yl)azetidin-2-ones as potential antileishmanial agents. Bioorg. Med. Chem. Lett. (2012) 22 5704–5706.

[18] A. Shaukat, H. M. Mirza, A. H. Ansari, M. Yasinzai, S. Z. Zaidi, S. Dilshad, F. L. Ansari, Benzimidazole derivatives: synthesis, leishmanicidal effectiveness, and molecular docking studies. Med. Chem. Res. 22 (2013) 3606-3620.

[19] B. Nare, J. Luba, L. W. Hardy, S. M. Beverley, New approaches to Leishmania chemotherapy: pteridine reductase 1 (PTR1) as a target and modulator of antifolate sensitivity. Parasitology 114 (1997) S101-S110

[20] D.G. Gourley, A.W. Schuettelkopf, G. A. Leonard, J. Luba, L.W. Hardy, S. M. Beverley, W. N. Hunter, Nat. Struct. Biol. 8 (2001) 521-525.

[21] Molecular Operating Environment (MOE 2012.10); Chemical Computing Group Inc., Montreal, Canada.

[22] E. F. Pettersen, T. D. Goddard, C. C. Huang, G. S. Couch, D. M. Greenblatt, E. C. Meng, T. E. Ferrin, UCSF Chimera--a visualization system for exploratory research and analysis. J. Comput. Chem. 25 (2004) 1605-1612.

[23] M. A. Kolosov, V. D. Orlov, V. V. Vashchenko, S. V. Shishkina, O. V. Shishkin, -Cinnamoyl- and 5-(ethoxycarbonyl)-6-styryl derivatives of 4-aryl-3,4-dihydropyrimidin-2(1H)-ones. Collect. Czech. Chem. Commun. 72 (2007) 1219–1228.

[24] M. A. Kolosov, V. D. Orlov, 5-Thiazolyl derivatives of 4-aryl-3,4-dihydropyrimidin-2(1h)-ones. Chem. Heterocycl. Comp. 44 (2008) 1418-1420.

[25] M. Baseer, F. L. Ansari, Z. Ashraf, Synthesis, in vitro antibacterial and antifungal activity of some n-acetylated and non-acetylated pyrazolines. Pak. J. Pharm. Sci. 26 (2013) 67-73.

[26] K. Jaspreet, D. Dube, R. Ramachandran, P. Singh, N. Singh, Thianthrene is a novel inhibitor of Leishmania donovani pteridine reductase 1 (PTR1) J. Mol. Biochem. 1 (2012) 68-75.

[27] K. Jaspreet, P. Kumar, S. Tyagi, P. Singh, R. Pathak, N. Singh, In silico screening, structure-activity relationship, and biologic evaluation of selective pteridine reductase inhibitors targeting visceral leishmaniasis. Antimicrob. Agents Chemother. 55 (2011) 659–666.

[28] P. Kumar, A. Kumar, S.S. Verma, N. Dwivedi, N. Singh, M.I. Siddiqi, R.P. Tripathi, A. Dube, N. Singh, Leishmania donovani pteridine reductase 1: Biochemical properties and structure-modeling studies. Exp Parasitol. 120 (2008):73-9.

[29] R.A. Prentis, Y. Lis, S. R. Walker, Pharmaceutical innovation by the seven UK-owned pharmaceutical companies (1964-1985). Br. J. Clin. Pharmacol. 25 (1988) 387-396.

[30] H. van de Waterbeemd, D. A. Smith, B. C. Jones, Lipophilicity in PK design: methyl, ethyl, futile. J. Comput. Aided Mol. Design 15 (2001) 273-286.

[31] http://www.drugbank.ca/drugs/DB00681

[32] D.A. Smith, Physicochemical properties in drug metabolism and pharmacokinetics, in Computer-assisted lead finding and optimization: current tools for medicinal chemistry, H. van de Waterbeemd, B. Testa, and G. Folkers, Editors. Wiley-VCH: Weinheim, Germany. (1997) 267

[33] W. J. Egan, Predicting ADME properties in drug discovery, in Drug design: structure- and ligand-based *appraoches*, K.M. Merz, D. Ringe, and C.H. Reynolds, Editors. Cambridge University Press: New York, USA. (2010) 165-173.

[34] J. R. Proudfoot, The evolution of synthetic oral drug properties. Bioorg. Med. Chem. Lett. 15 (2005) 1087-1090.

[35] S.A. Hitchcock, Structral modification that alter the P-glycoprotein eflux properties of compounds. J. Med. Chem. 55 (2012) 4877-4895.

[36] Y. R. Prasad, A. S. Rao, R. Rambabu, Synthesis of Some 4'-Amino Chalcones and their Antiinflammatory and Antimicrobial Activity. Asian J. Chem. 21 (2009) 907-914.

[37] Marvin 6.0.0, 2013, (http://www.chemaxon.com)

[38] H. van de Waterbeemd, E. Gifford, ADMET in silico modelling: towards prediction paradise? Nat. Rev. Drug Discovery 2 (2003) 192-204.

**Figure Legends**

**Figure1:** Computer generated molecular models of Compound **8** (gold) superimposed on MTX (purple) docked into the binding site of PTR1 (A) Overall structure (B) Close-up view with important interactions (C) & (D) 2D ligand interaction maps of MTX and compound 8 respectively.

**Figure 2:** (A-C) 2D ligand interaction maps of compounds of Series 1 docked into the binding site of PTR1.

**Figure 3:** a) Superposition of the best conformations of Compound **8e** (Reddish brown ) and **8i** (magenta) into the binding site of PTR1.

**Figure 4:** 2D ligand interaction maps of weakly active compounds (A) compound **8a** (B) compound **8h**.

**Figure 5:** Docking of **12c** in the active site of PTR1 a) 3D view b) 2D ligand interactions

**Figure 6:** Total polar surface area depicted as TPSA of the compounds calculated by Marvin 6.0.0 of Chemaxon Software.

**Figure 7:** LogD values at various physiological pH. a) compounds of SAR series 1; 2) Compounds of SAR series 2

**Figure 8:** (a) and (b) depicts the relation between logD and renal clearances Cl in mg/ml/min. (c) Renal clearance in increasing trend of logD. (d) Increasing trend in renal clearance due to pharmacokinetic factors as MW, TPSA, HBD count (outer ring) as percentile. Highest clearance (24%) shown by lead compound **8i** (inner ring).

**Table 1.**

*In vitro* antileishmanial activity of dihydropyrimidines (**1-13**)

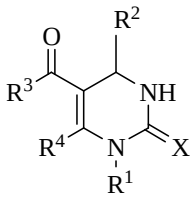


**1-13**

| Compound | $R^1$ | $R^2$ | $R^3$ | $R^4$ | X | $IC_{50}$ (µg/mL) ±SEM |
|---|---|---|---|---|---|---|
| **1** | H | $C_6H_5$ | OEt | Me | O | 0.99±0.03 |
| **2** | $CH_2.C_6H_5$ | $C_6H_5$ | OEt | Me | O | 0.99±0.02 |
| **3** | H | $C_6H_5$ | Me | Me | O | 0.61±0.01 |
| **4** | H | 3-$NO_2.C_6H_4$ | Me | Me | O | 0.67+0.04 |
| **5** | H | 3-Me.$C_6H_4$ | Me | Me | O | 0.89±0.01 |
| **6** | H | 3-OMe,4-OH.$C_6H_3$ | Me | Me | O | 0.71±0.01 |
| **7** | H | 4-OMe.$C_6H_4$ | Me | Me | O | 0.69±0.01 |
| **8** | Me | $C_6H_5$ | Me | Me | O | 0.63±0.02 |
| **9** | H | 3-$NO_2.C_6H_4$ | $OCHMe_2$ | Me | O | 0.74±0.04 |
| **10** | H | 3-$NO_2.C_6H_4$ | OMe | $CH_2OMe$ | O | 0.95±0.02 |
| **11** | H | $C_6H_5$ | Me | Me | S | 0.78±0.02 |
| **12** | H | 4-Me.$C_6H_4$ | OEt | Me | S | 0.63±0.01 |
| **13** | H | 3-OH.$C_6H_4$ | OEt | Me | S | 0.65+0.04 |
| **Amphoterecin B (Standard drug)** | | | | | | **0.56±0.01** |

**Table 2.** SAR exploration around DHPM analogues (**8a-8i**)

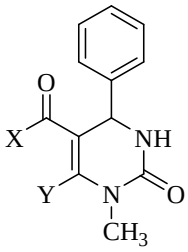


**8a-i**

| Compound | X | Y | $IC_{50}$ (µg/mL) ±SEM | |
|---|---|---|---|---|
| | | | *L. major* | *L. donovani* |
| **8a** | 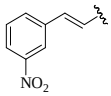 | $CH_3$ | 0.73±0.04 | NI |
| **8b** | 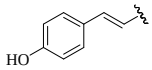 | $CH_3$ | 0.59±0.05 | NI |
| **8c** | 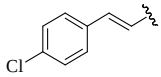 | $CH_3$ | 0.63±0.04 | NI |
| **8d** | $CH_3$ | 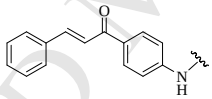 | 0.54±0.01 | >100 |
| **8e** | $CH_3$ | 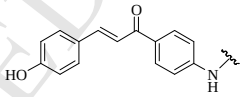 | 0.51±0.06 | 7.5 |
| **8f** | $CH_3$ | 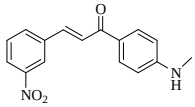 | 0.67±0.05 | >100 |
| **8g** | $CH_3$ | 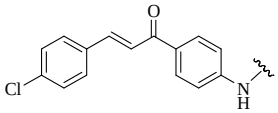 | 0.53±0.04 | 4.40±0.98 |
| **8h** | $CH_3$ | 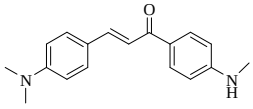 | 0.71±0.01 | NI |
| **8i** | - | 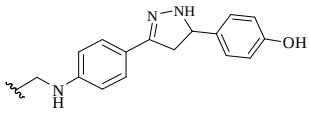 | 0.47±0.02 | **1.5±0.17** |
| **Amphoterecin B** | | | **0.56±0.01** | |
| **SSG (sodium stibogluconate)** | | | **-** | **2.98** |

SEM=Standard error of the mean; NI=No inhibition

**Table 3.** SAR exploration around thioxo-analogues (**12a-d**)

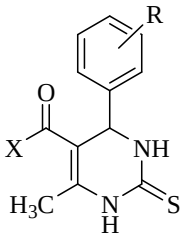


**12a-d**

| Compound | X | R | IC$_{50}$ (µg/mL) ±SEM | |
|---|---|---|---|---|
| | | | *L. major* | *L. donovani* |
| **12a** | 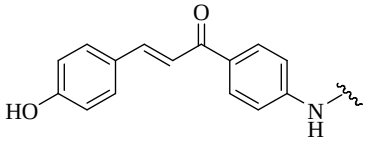 | 4-$CH_3$ | 0.53±0.03 | NI |
| **12b** | 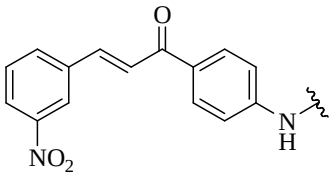 | 4-$CH_3$ | 0.65±0.01 | NI |
| **12c** | 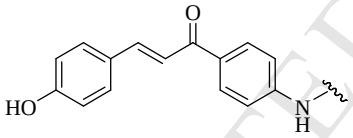 | 3-OH | 0.51±0.04 | 5.58±1.1 |
| **12d** | 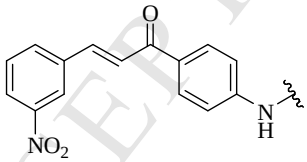 | 3-OH | 0.58±0.01 | NI |
| | **Amphoterecin B** | | **0.56±0.01** | - |
| | **SSG (sodium stibogluconate)** | | - | **2.98** |

SEM=Standard error of the mean; NI=No inhibition

**Table 4:**

Descriptors of synthesized compounds

| Comp. | logP MOE | logD7.4 | Sw mg/ml | LogPer | TPSA $A^2$ | HBA | HBD | NOR | Cl ml/min/kg | MW Da | logK | Allowed MW range | Oral Bioavailability |
|---|---|---|---|---|---|---|---|---|---|---|---|---|---|
| **8a** | 3.77 | 3.36 | 0.0045 | -10.2294 | 187.879 | 7 | 1 | 5 | 0.10485 | 377.4 | -1.124 | 400-450 | less 50% |
| **8b** | 3.49 | 3.1 | 0.0143 | -9.1511 | 157.403 | 5 | 2 | 4 | 0.1848 | 348.4 | -0.852 | 350-400 | S. less |
| **8c** | 4.39 | 4.02 | 0.0048 | -6.8452 | 107.21 | 4 | 1 | 4 | 0.0939 | 366.85 | -1.175 | 450-500 | >50% |
| **8d** | 4.78 | 3.89 | 0.0015 | -8.4391 | 162.639 | 6 | 2 | 8 | 0.1052 | 465.55 | -1.123 | 450-500 | >50% |
| **8e** | 4.48 | 3.58 | 0.0022 | -10.408 | 211.401 | 7 | 3 | 8 | 0.1309 | 481.55 | -1.019 | 450-500 | >50% |
| **8f** | 4.76 | 3.83 | 0.0007 | -11.675 | 246.272 | 9 | 2 | 9 | 0.0957 | 510.55 | -1.166 | 450-500 | less 50% |
| **8g** | 5.38 | 4.5 | 0.0007 | -8.2351 | 164.301 | 6 | 2 | 8 | 0.0725 | 499.99 | -1.294 | 450-500 | >50% |
| **8h** | 4.7 | 4 | 0.0016 | -9.8329 | 203.068 | 7 | 2 | 9 | 0.0897 | 508.62 | -1.196 | 450-500 | S. less |
| **8i** | 4.12 | 2.53 | 0.0043 | -10.5468 | 217.243 | 8 | 4 | 7 | 0.4266 | 495.58 | -0.401 | 350-400 | less 50% |
| **12a** | 5.14 | 4.95 | 0.0003 | -6.5709 | 122.55 | 4 | 4 | 7 | 0.103 | 483.59 | -1.134 | >500 | >50% |
| **12b** | 5.42 | 5.2 | 0.0001 | -7.4393 | 148.14 | 3 | 3 | 8 | 0.081 | 512.59 | -1.245 | >500 | >50% |
| **12c** | 4.86 | 4.14 | 0.0002 | -7.1931 | 142.78 | 4 | 4 | 8 | 0.098 | 514.56 | -1.153 | 450-500 | >50% |
| **12d** | 4.58 | 4.38 | 0.0008 | -8.52543 | 168.37 | 5 | 5 | 7 | 0.089 | 485.56 | -1.195 | 450-500 | >50% |
| **Ampho** | 0.71 | -2.31 | 0.0149 | -11.516 | 319.61 | 17 | 13 | 3 | 0.091 | 924.09 | -1.279 | <300 | less 50% |

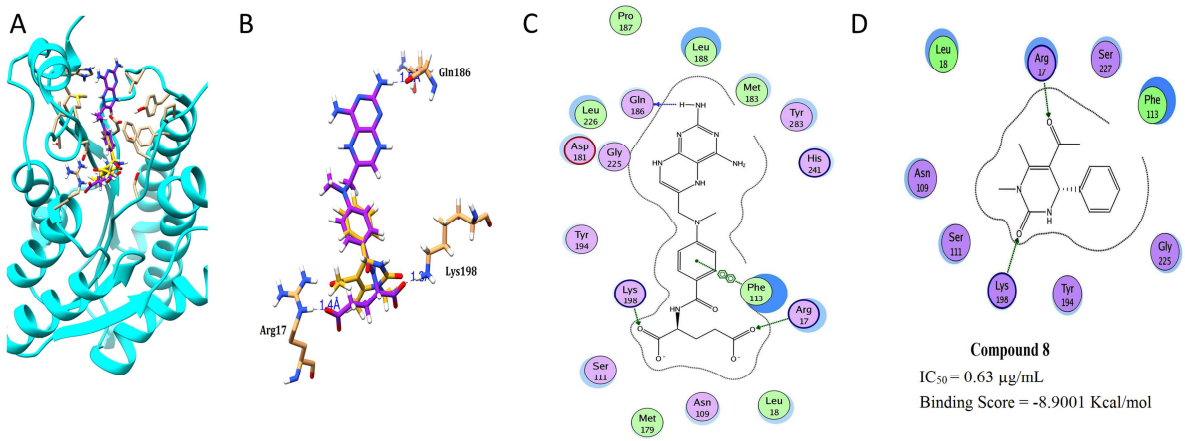

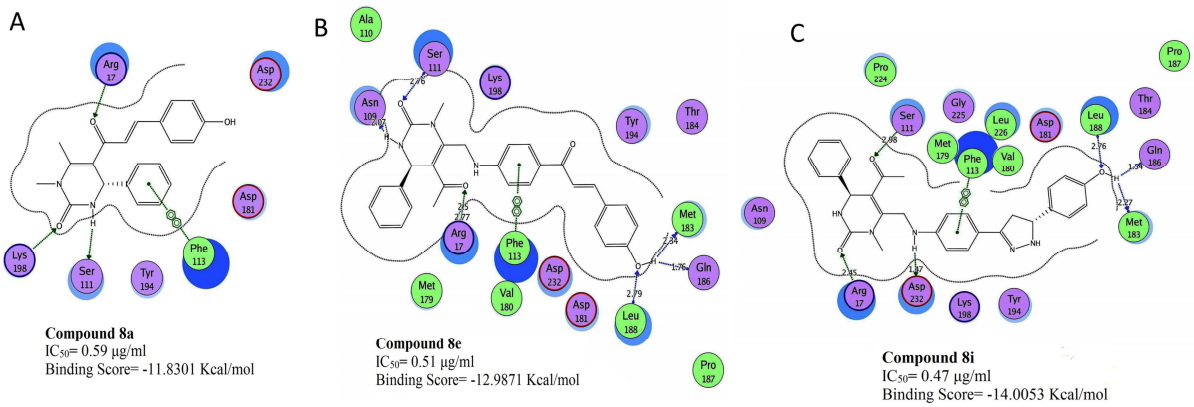


**Compound 8a**
$IC_{50}$= 0.59 µg/ml
Binding Score= -11.8301 Kcal/mol

**Compound 8e**
$IC_{50}$= 0.51 µg/ml
Binding Score= -12.9871 Kcal/mol

**Compound 8i**
$IC_{50}$= 0.47 µg/ml
Binding Score= -14.0053 Kcal/mol

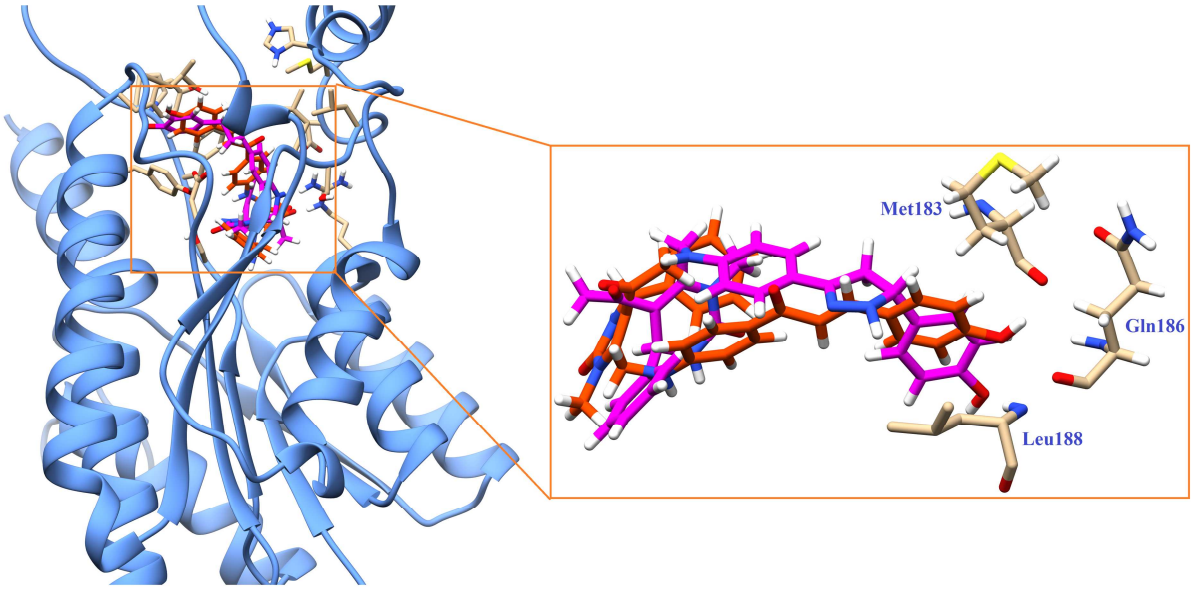

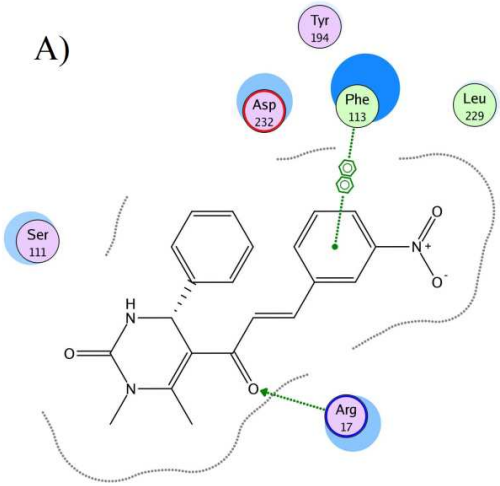


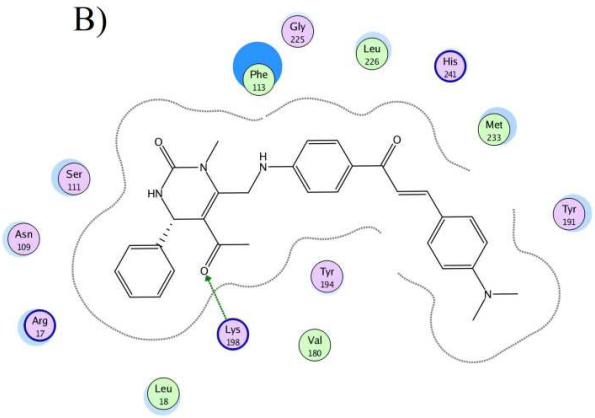

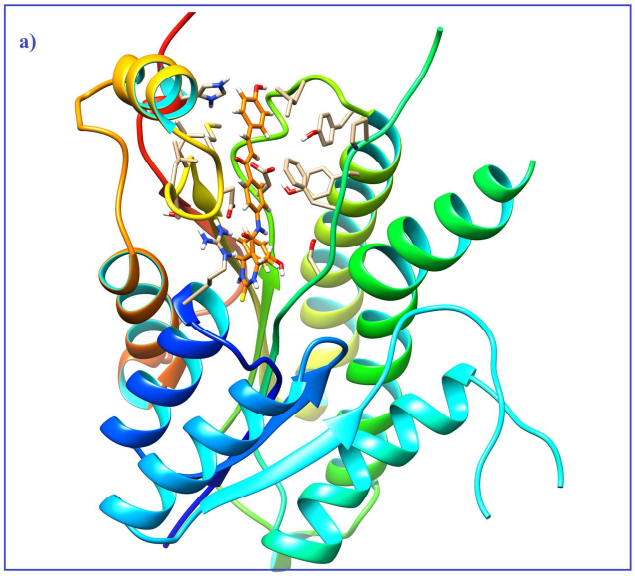


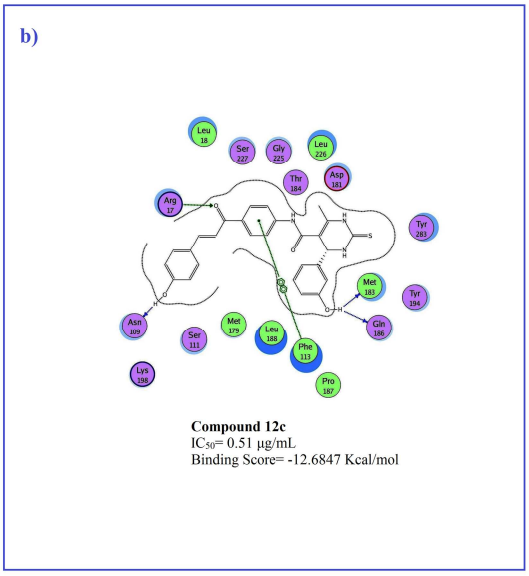

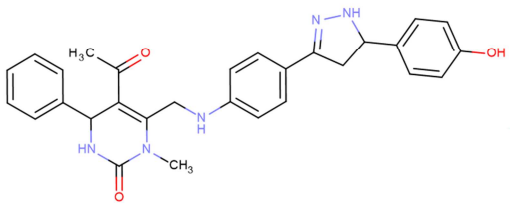

TPSA 106.06 A²

7.4pH

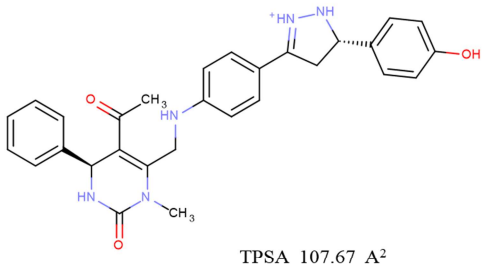

TPSA 107.67 A²

**Lead compound 8i**

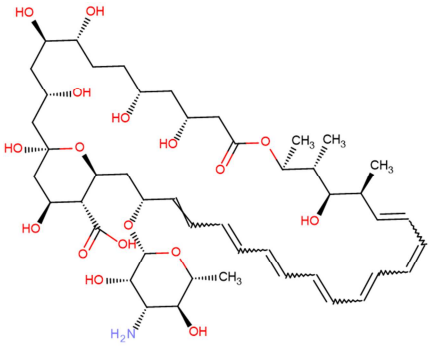

TPSA 319.61 A²

7.4pH

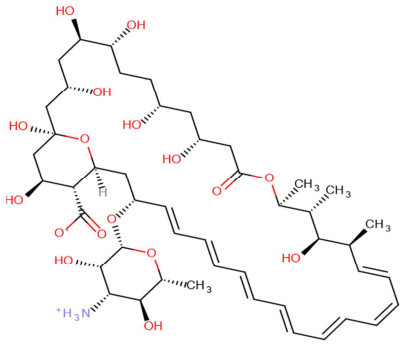

TPSA 324.06 A²

**Amphotericin B**

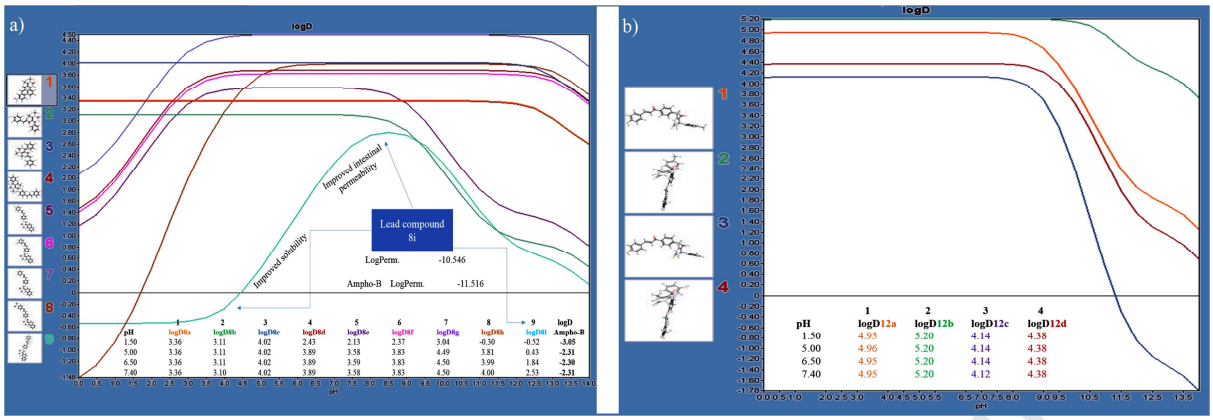

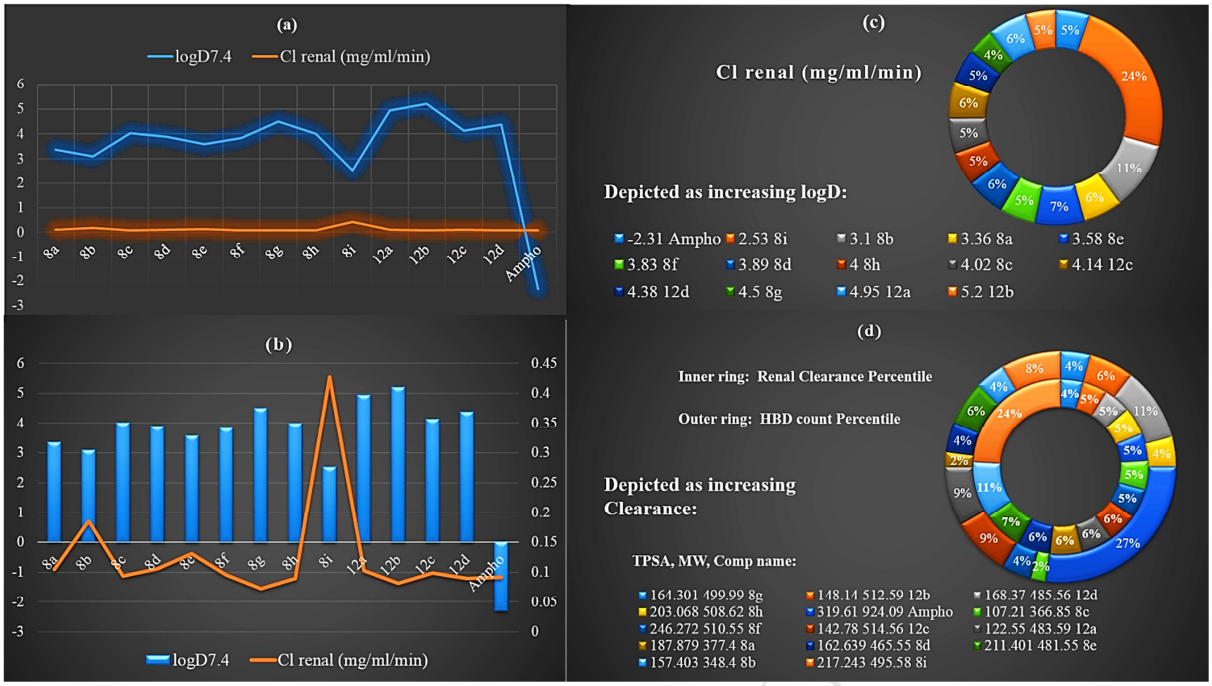

# Schemes

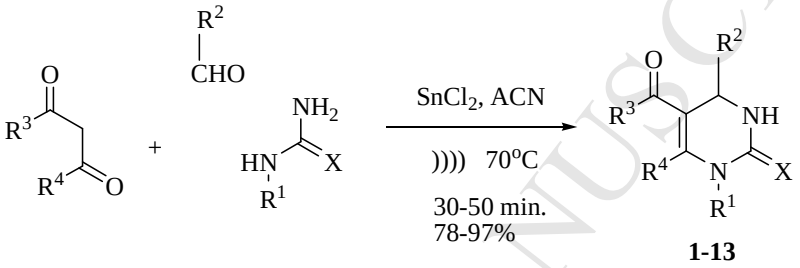


**Scheme 1**. Synthesis of dihydropyrimidines **1-13**

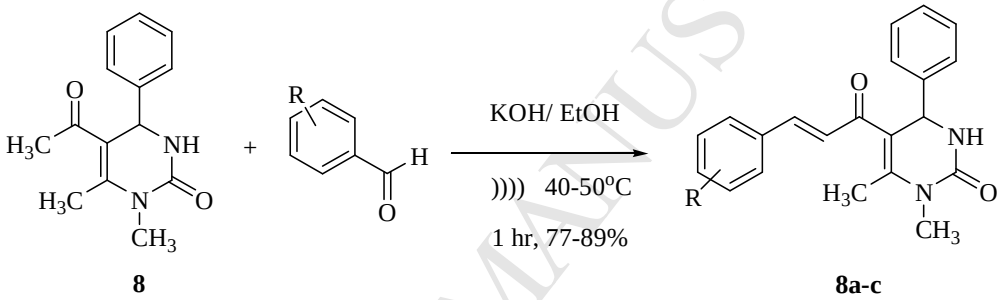


**Scheme 2**. Synthesis of chalcones from dihydropyrimidines

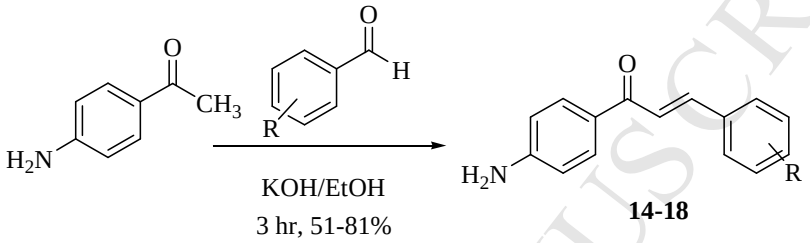


**Scheme 3a**. Synthesis of 4-amino chalcones

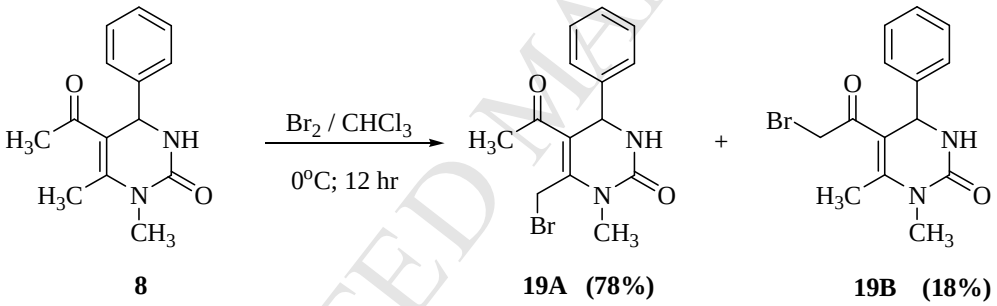


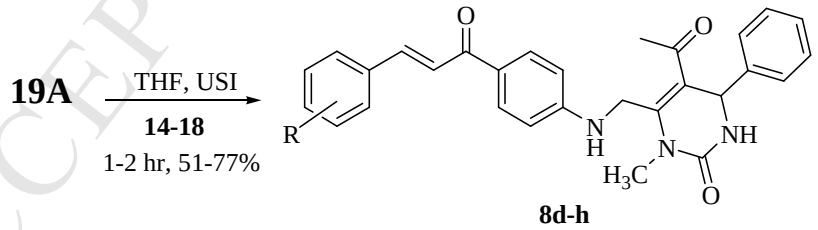


**Scheme 3b**. SAR exploration around DHPM 8 at C-6 position

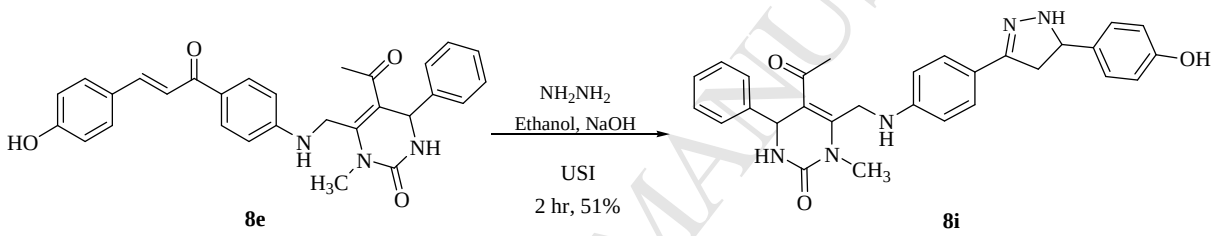


**Scheme 4**. Synthesis of pyrazoline (**8i**) from chalcone **8e**

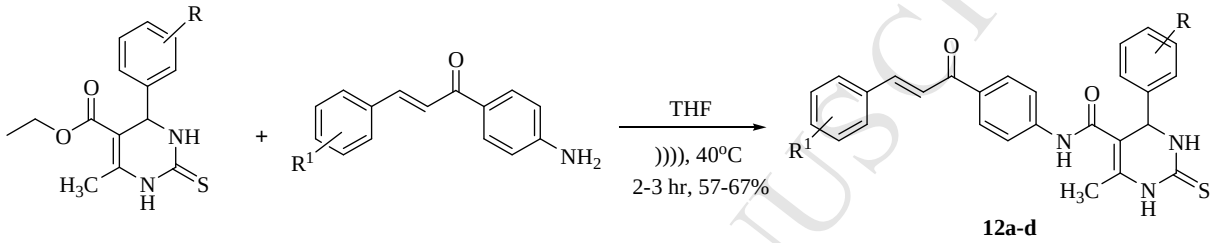


**Scheme 5**. SAR exploration around thioxo-analogues **12** and **13** at C-5 position

# Highlights

- Structure based C-5 and C-6 modifications of 3,4-dihydropyrimidine core.
- Modifications were found to have enhanced *in vitro* inhibition potential
- Compound **8i** showed potent *in vitro* antileishmanial activity.
- Molecular docking analysis was carried out
- Drug-like properties was evaluated through *in silico* ADMET predictions